

T-2038

EXPERIMENTAL APPARATUS
FOR THE STUDY OF GAS ADSORPTION
ON SPENT SHALE

by
Joseph L. Zuech

ProQuest Number: 10782151

All rights reserved

INFORMATION TO ALL USERS

The quality of this reproduction is dependent upon the quality of the copy submitted.

In the unlikely event that the author did not send a complete manuscript and there are missing pages, these will be noted. Also, if material had to be removed, a note will indicate the deletion.



ProQuest 10782151

Published by ProQuest LLC (2018). Copyright of the Dissertation is held by the Author.

All rights reserved.

This work is protected against unauthorized copying under Title 17, United States Code
Microform Edition © ProQuest LLC.

ProQuest LLC.
789 East Eisenhower Parkway
P.O. Box 1346
Ann Arbor, MI 48106 – 1346

A thesis submitted to the Faculty and the Board of Trustees of the Colorado School of Mines in partial fulfillment of the requirements for the degree of Master of Science-- Chemical and Petroleum Refining Engineering.

Signed: Joseph L. Zuech
Joseph L. Zuech

Golden, Colorado

Date: March 9, 1978

Approved: A.L. Hines
A.L. Hines
Thesis Advisor

E.D. Sloan, Jr.
E.D. Sloan, Jr.
Thesis Advisor

P.F. Dickson
P.F. Dickson
Head of Department

Golden, Colorado

Date: March 9, 1978

ABSTRACT

An experimental apparatus capable of determining accurate adsorption isotherms was designed, constructed, and tested. The adsorption isotherms for methane in Linde 5A molecular sieve were determined gravimetrically using a Cahn R-100 electrobalance. This apparatus is somewhat unique because isotherms can be measured gravimetrically from the vacuum region to 100 psia.

The pressure is measured with two thermistor gauges, a pressure transducer with digital readout, a Wallace and Tiernan gauge and a discharge vacuum gauge. Temperature is measured with Tagliabue thermometers.

A step by step operating procedure for the apparatus is presented for future use by operators. Future operators will use samples of spent or raw oil shale as the adsorbent.

Isotherms were measured at three temperatures so that adsorption isosteres could be determined and the data checked for internal consistency. The results were reproducible to within two percent. The isotherms were compared with those obtained by earlier investigators.

TABLE OF CONTENTS

ARTIFUR LAKES LIBRARY
 COLORADO SCHOOL of MINES
 GOLDEN, COLORADO 80401

ARTIFUR LAKES LIBRARY
 CO

	<u>Page</u>
LIST OF FIGURES -----	v
LIST OF TABLES -----	vii
LIST OF SYMBOLS -----	viii
INTRODUCTION -----	1
LITERATURE SURVEY -----	3
Adsorption Equilibrium Studies -----	3
Theory -----	4
SYSTEM SELECTION -----	13
EXPERIMENTAL DESIGN -----	17
SYSTEM CALIBRATION AND PERFORMANCE -----	29
EXPERIMENTAL PROCEDURE -----	37
Regeneration of Adsorbent -----	37
Collecting Data -----	39
Vacuum System Shutdown -----	39
Bouyancy Tests -----	41
RESULTS -----	45
DISCUSSION -----	60
CONCLUSIONS -----	71
RECOMMENDATIONS -----	73
APPENDICES -----	74
A. Data and Calculated Results -----	74
B. Error Analysis -----	82
C. Sample Calculations -----	85
D. Calibration Reports -----	89
BIBLIOGRAPHY -----	97

LIST OF FIGURES

	<u>Page</u>
Figure 1. Schematic Diagram of Gravimetric Adsorption Apparatus -----	18
2. Schematic Diagram of the Control Panel for the Gravimetric Adsorption Apparatus ----	19
3. Diagram of Adsorption Vessel -----	20
4. Diagram of Cahn Model R-100 Electrobalance --	22
5. Cahn Model R-100 Electrobalance Thermocouple Connection Diagram -----	23
6. Wiring Diagram for the Pressure Transducers--	27
7. Weight Drift with Temperature -----	30
8. Calibration Curve for 25 psia Transducer Using Mercury Manometer -----	32
9. Calibration Curve for 250 psia Transducer Using Mercury Manometer -----	33
10. Calibration Curve for 250 psia Transducer Using Dead Weight Tester -----	34
11. Bouyancy Test Conducted at 298°K -----	43
12. Adsorption Isotherm for Methane on 5A Crystals at 273°K -----	46
13. Adsorption Isotherm for Methane on 5A Crystals at 298°K -----	47
14. Adsorption Isotherm for Methane on 5A Crystals at 308°K -----	48
15. Comparison of Methane Adsorption Isotherms on 5A Crystals and Powder at 273°K -----	49

List of Figures continued

	<u>Page</u>
Figure 16. Comparison of Methane Adsorption Isotherms on 5A Crystals and Pellets at 298°K-----	50
17. Adsorption Isosteres at Various Loadings -----	51
18. Characteristic Curve Plotted in the Form $\ln W$ Versus ϵ^2 For Methane Adsorption on 5A Crystals -----	53
19. Plot of $P/V (P_0 - P)$ Versus P/P_0 for 298°K Data on 5A Crystals (Test for BET Isotherm Fit) -----	55
20. Plots of $1/P$ Versus $1/C$ for 273, 298, and 308°K Data on 5A Crystals (Test for Langmuir Isotherm Fit) -----	56
21. Plots of $\log C$ Versus $\log P$ for 273, 298, and 308°K Data on 5A Crystals (Test for Freundlich Isotherm Fit) -----	57
22. Low Pressure Isotherms Fit by Ruthven's Model -----	58
23. High Pressure Isotherms Fit by Ruthven's Model -----	59
24. Comparison of 273°K Isotherm Data on 5A Crystals -----	61
25. Plot of $\ln K$ vs. $1/T$ Used to Compare Henry's Law Constants -----	66
26. Middle Pressure Range Isotherms Fit by Ruthven's Model -----	68
27. Methane Adsorption on 5A Crystals at 298°K Fit With Ruthven's Model Using Effective Molecular Volume-Pressure Relationship Determined from this Study -----	69
28. Methane Adsorption on 5A Crystals a 308°K Fit With Ruthven's Model Using Effective Molecular Volume-Pressure Relationship Determined from this Study -----	70

LIST OF TABLES

	<u>Page</u>
Table 1. Pressure Leak Test -----	36
2. Variation of Isosteric Heat of Adsorption with Loading -----	52
3. Comparison of High Pressure Data with Rolniak's Data -----	63
4. Comparison of the Statistical Thermodynamic Model Parameters Determined from the Data of this Study with those Obtained from the Data of Loughlin and Rolniak -----	65
AI. Adsorption of Methane on 5A Crystals at 273°K (Run 16) -----	74
AII. Adsorption of Methane on 5A Crystals at 298°K (Run 17) -----	75
AIII. Adsorption of Methane on 5A Crystals at 308°K (Run 18) -----	76
AIV. Adsorption of Methane on 5A Powder at 273°K (Run 12) -----	77
AV. Adsorption of Methane on 5A Pellets at 298°K (Run 15) -----	78
AVI. Bouyancy Test at 273°K -----	79
AVII. Bouyancy Test at 298°K -----	80
AVIII. Bouyancy Test at 308°K -----	81

LIST OF SYMBOLS

B	= adsorbate structural constant (mol/Kcal)
B°	= function of reduced temperature (dimensionless)
B'	= function of reduced temperature (dimensionless)
b	= effective molecular volume ($\text{Å}^3/\text{molecule}$)
b ₁	= first Langmuir constant (dimensionless)
b ₂	= second Langmuir constant (psia^{-1})
C	= bouyancy correction term (μg)
c	= equilibrium sorbate concentration (mmoles/g)
\bar{c}	= equilibrium sorbate concentration (molecules/cavity)
f	= equilibrium fugacity of the sorbed species (atm)
f _s	= saturation fugacity of the pure liquid sorbate (atm)
I	= intercept (unitless)
K	= Henry's Law constant (molecules/cavity torr)
k	= temperature dependent quantity that is a constant in the Freundlich equation (dimensionless)
M	= Molecular weight (g/gmole)
m	= saturation limit (dimensionless)
m _a	= actual mass (μg)
m _m	= measured mass (μg)
m _r	= regenerated mass (μg)
m _s	= mass of sample (μg)
N _O	= Avogadro's number, (6.02×10^{23} molecules/mole)
n	= temperature dependent quantity that is a constant in the Freundlich equation (dimensionless)

List of Symbols continued

P	= pressure of the gas (psia)
P _C	= critical pressure (atm)
P _O	= saturation pressure of pure adsorbate (atm)
P _R	= reduced pressure (dimensionless)
S	= slope (dimensionless)
R	= gas constant
T	= temperature (°K)
T _C	= critical temperature (°K)
T _R	= reduced temperature (dimensionless)
V	= volume (cc)
V _C	= effective counterweight volume (cc)
v	= molar volume (cc/gmole)
v'	= volume of α cage of a specific zeolite (Å ³)
v _m	= volume of one monomolecular layer of gas ($\frac{cc}{g}$)
v _S	= volume per mole of gas at standard conditions (22,400 cc/gmole)
W	= filled volume of adsorption space ($\frac{cc}{g}$)
W _O	= limiting pore volume ($\frac{cc}{g}$)
Z	= compressibility factor (dimensionless)
α	= projected area of a molecule on the surface when the molecules are arranged in close two dimensional packing (cm ² /molecule)
ε	= adsorption potential (Kcal/gmole)
ρ	= density (g/cc)
ρ _g	= density of the gas (μg/cc)

List of Symbols continued

ρ_i = density of the adsorbed substance (g/cc)

ρ_s = density of the sample ($\mu\text{g}/\text{cc}$)

ρ_x = density of the gas phase (g/cc)

ϕ = fugacity coefficient (dimensionless)

θ = volume of adsorbed phase (cc)

ω = accentric factor (dimensionless)

ACKNOWLEDGEMENTS

The author wishes to express his appreciation for the support provided by the United States Energy Research and Development Administration, Contract Number E(29-2)-3780.

Grateful appreciation is extended to Professors Earl D. Sloan, Jr., and Anthony L. Hines, thesis co-advisors, for their guidance, understanding, and patience during this study. I would also like to acknowledge the help Ron Miner, C.P.R. Department technician, contributed in the wiring of the apparatus. Sincere thanks is extended to the Master of Science Committee members: Professors Arthur J. Kidnay and Phillip F. Dickson. Finally, I would like to thank my family for their patience and encouragement throughout my graduate work.

INTRODUCTION

Two major processes are used to produce oil from oil shale. In situ processing involves heating the underground formation to extract the oil, while the above ground retorting process requires that the shale be mined first. The in situ process also eliminates spent shale disposal problems. For these two reasons in situ processing seems to be the most attractive of the two processes. To better understand the in situ process it is necessary to investigate the adsorptive properties of the hydrocarbon and combustion gases produced (1).

The purpose of this project was to design and construct an experimental apparatus capable of measuring adsorption isotherms gravimetrically. The apparatus was designed to operate within a pressure range of 6×10^{-4} torr to 100 psia and a temperature range of -20 to 400°C.

The system was tested by conducting measurements on a previously studied system. Linde 5A molecular sieve was chosen as the sorbent because it consists of well-defined cavities within which the sorbate molecules are occluded. Only physical adsorption occurs and there should not be any hysteresis. Methane was the adsorbate.

Future investigators will use the apparatus to study single and binary component gas adsorption on spent oil shale. The raw shale samples were obtained from the Energy Research and Development Administration in Laramie, Wyoming.

This thesis presents a complete description of the apparatus. All design aspects are explained. Isotherms are presented and their accuracy discussed. The isosteric heat of adsorption is estimated and compared with literature values. Complete calibration data and an operating procedure for the apparatus is provided.

LITERATURE SURVEY

A large amount of literature on solid-gas adsorption has been published. Only selected publications are reviewed here with emphasis on applicability to the present work. General references on physical adsorption have been published by Young and Crowell (2) and Brunauer (3).

Adsorption Equilibrium Studies

The sorption of methane on 5A zeolite has not been studied extensively. Ruthven and Loughlin (4, 5, 6) and Kidnay and Hiza (7) performed studies at low pressures (<700 torr) and low temperatures ($\leq 273^{\circ}\text{K}$). Lederman (8) obtained methane sorption data on 5A pellets at 175, 195, and 295°K at pressures ranging from 6 to 50 atmospheres. Rolniak's (9) data was collected at temperatures of 288, 298, and 308°K and at pressures ranging from 50 to 1300 psia.

Ruthven and Loughlin were able to fit their data to their statistical thermodynamics model. An apparatus similar to the one used in this study was utilized. The low pressure data of this study at 273°K is compared with their data. The low pressure data at 273, 298, and 308°K was fit with their model.

Rolniak used elution chromatography with a radioactive tracer to obtain his isotherms. He was able to fit his data with Ruthven's model after adjusting one of the parameters, the effective molecular volume. This was not surprising since Ruthven had already suggested that there might be a decrease in effective molecular volume with increasing pressure (10). The high pressure data at 298 and 308°K was compared with Rolniak's data.

The data of Rolniak shows results opposite than expected when compared with the high pressure volumetric data of Lederman. Lederman's data points at 295°K lie below those of Rolniak at 298°K. Rolniak explains this discrepancy by pointing out that Lederman did not maintain good temperature control and had less severe regeneration conditions.

Theory

Adsorption processes are classified as physical or chemical. Physical adsorption, also known as van der Waals adsorption, is brought about by intermolecular forces. The physically adsorbed layer is formed in much the same manner as a liquid is formed when a vapor is condensed. Physically adsorbed layers many molecular diameters thick behave like two-dimensional liquids. Chemical adsorption involves the transfer of electrons between the solid and the gas. This means that chemical adsorption leads to the formation of a monolayer and that chemisorption is more irreversible than physical adsorption.

Adsorption is a spontaneous process, and therefore, the free energy of the system decreases. The entropy also decreases because the adsorbed molecules have lost a degree of freedom in moving from the gas phase to the adsorbed phase. It follows from the equation

$$\Delta H = \Delta G + T \Delta S$$

that the adsorption process must always be exothermic. The decrease in heat content of the system is called the heat of adsorption. In physical adsorption the heat of adsorption is of the same order of magnitude as the heats of condensation of gases; in chemisorption the heat of adsorption is the same order of magnitude as the heat of chemical reaction.

Adsorption equilibrium data can be analyzed by plotting the amount adsorbed as a function of pressure at constant temperature. This is known as an adsorption isotherm.

Adsorption isosteres are plots of pressure as a function of temperature at a constant amount adsorbed. These are obtained indirectly from a family of adsorption isotherms. The isosteres can be plotted in the form $\log p$ versus $1/T$ to yield a family of straight lines, each corresponding to a constant value of the amount adsorbed. The linearity of the isosteres provide a check on the internal consistency of the isotherms. The slopes of the isosteres give the heats of adsorption at each amount adsorbed, using the Clausius-Clapeyron equation in the form

$$d \ln p / d(1/T) = -q_{st} / R \quad (1)$$

Here q_{st} is the isosteric heat of adsorption. Plots of isosteric heat of adsorption versus amount adsorbed can be used in characterizing the nature of the adsorbent surface and the degree of lateral interaction.

Three approaches are generally used to correlate isotherm data on zeolites. One is a surface phenomenon approach. The second is a purely empirical approach, and the third is a pore volume filling approach. These three approaches will be applied in a manner similar to the one Loughlin (4) used in correlating his sorption data on zeolites.

The surface phenomenon approach interprets data by first assuming the nature and mobility of the adsorbed phase and then deriving a theoretical isotherm equation, as done by Langmuir (11) in 1915. His theory assumes the following behavior:

- a) The interaction between adsorbed molecules is negligible.
- b) Adsorption takes place only through collisions of gas molecules with vacant sites. Those striking other molecules on the surface are elastically reflected.
- c) A monolayer is formed.

The equation that Langmuir derived based on these assumptions is:

$$c = (b_1 p) / (1 + b_2 p) \quad (2)$$

where: b_1 is the first Langmuir Constant, dimensionless, b_2 is the second Langmuir Constant, psia^{-1} , p is the pressure of the gas, psia , and c is the equilibrium adsorbate concentration, mmoles/gm .

To determine whether the experimental data obeys the Langmuir isotherm equation, the equation must first be rearranged into linear form:

$$1/c = (1/b_1)(1/p) + (b_2/b_1)$$

A plot of $1/c$ versus $1/p$ should give a straight line with slope $1/b_1$ and intercept b_2/b_1 if the data follows Langmuir's isotherm. The fact that the data gives a straight line is a necessary but not sufficient condition to prove that the Langmuir assumptions are valid. The theory must also predict the heat content or the temperature dependence of the isotherm (12).

The oldest isotherm equation is the Freundlich equation (3). This equation is purely empirical in that it is an analytical expression for the experimental data. The Freundlich isotherm equation is:

$$c = k(p)^{1/n}, \quad n > 1 \quad (3)$$

where k and n are quantities dependent on temperature. The Freundlich equation written in linear form is:

$$\log c = \log k + (1/n)\log p$$

A plot of $\log c$ versus $\log p$ should give a straight line with the slope equal to $1/n$ and the intercept equal to $\log k$ if the data obeys the Freundlich equation.

The Dubinin-Polanyi theory of pore volume filling has its origin in the potential theory of Polanyi (3, 13, 14, 15). The Polanyi theory assumptions are;

- a) The adsorbent exerts a strong long range attractive force that gives rise to adsorption.
- b) The adsorbate follows the same equation of state whether it is adsorbed or in the gas phase.
- c) The adsorption potential is similar to the gravitational potential.
- c) The reduced curve $\epsilon = f(\phi)$ is the same for all temperatures and is known as the characteristic curve. The parameter, ϵ , is the adsorption potential and θ is the adsorbed phase volume.

The forces of attraction are large enough to form many adsorbed layers. These layers are in a state of compression. The compression is greatest on the first adsorbed layer and decreases to the density of the surrounding gas at the outermost layer. An analogy can be drawn with the atmosphere surrounding the earth.

Polanyi defined the potential for adsorption as the work done in bringing a molecule from the gas phase to the adsorbent. This work is known as the work of compression as is given by

$$\epsilon_i = \int_{\rho_x}^{\rho_i} V dP$$

ARTHUR LAKES LIBRARY
 COLORADO SCHOOL of MINES
 GOLDEN, COLORADO 80401

ϵ_i is the adsorption potential at a point where the density of the adsorbed substance is ρ_i , ρ_x is the density in the gas phase, and $V = M/\rho$, where M is the adsorbate molecular weight. Polanyi assumed that the gas obeys the same equation of state in the adsorbed phase as in the gas phase because this integral cannot be evaluated unless the volume or density can be determined as a function of the pressure both in the gas phase and in the adsorbed phase. He based his assumption on the similarity between physical adsorption and condensation. The success of Polanyi's theory indicates that this is not a bad assumption.

Dubinin combined Polanyi's potential theory with his pore volume filling approach to arrive at the Dubinin-Polanyi theory. Dubinin proposed that the pores of the adsorbent are filled in much the same manner as fluid fills a container. One advantage of this theory is that there aren't any detailed assumptions regarding the sorbed gas, but is based on general postulates that have been verified experimentally for microporous sorbent systems.

Dubinin describes the state of the adsorbed substance as essentially similar to that of the corresponding bulk liquid. The adsorption potential is, therefore, the difference in free energy between the adsorbed species and the corresponding saturated liquid,

$$\epsilon = \Delta G = RT \ln(f/f_s) \quad (4)$$

where f is the equilibrium fugacity of the sorbed species and f_s is the saturation fugacity of the pure liquid sorbate. Recalling that the adsorption potential is independent of temperature and depends only on the filled volume of the adsorption space.

$$\Delta G = f(W) \quad (5)$$

where

$$W = cv$$

W = filled volume of adsorption space, cc/gm.

c = sorbate concentration, mmoles/gm.

v = molar volume of sorbate cc/mmole.

The characteristic curve is a test for checking the consistency of data obtained at two different temperatures. If the points lie on the same curve, the data can be said to be consistent.

The characteristic curve representation as investigated by Dubinin et al (16, 17, 18) can be used to correlate isotherms for a particular adsorbent over a wide range of

temperatures utilizing only one set of constants. The correlation equation is given by:

$$W = W_0 \exp (-\beta \epsilon^2) \quad (6)$$

where W = adsorbed volume, cm^3/g

W_0 = limiting pore volume, cm^3/g

β = adsorbate structural constant $(\text{mol}/\text{Kcal})^2$

ϵ = adsorption potential, Kcal/mole

This equation can be rearranged to linear form and a plot of $\ln(W)$ versus ϵ^2 should be linear.

The pore volume filling approach was also utilized by Ruthven in developing a simple theoretical isotherm that describes cavity filling in terms of statistical thermodynamics (10). Ruthven's assumptions are

- a) Adsorbed molecules are confined within particular cavities of the zeolite lattice but not adsorbed at specific localized sites within a cavity.
- b) When two or more molecules occupy the same cavity, the molecular interaction is represented simply as a reduction in free volume due to the finite size of the molecules. Attractive interactions between sorbate molecules and interaction between molecules in different cages are neglected.
- c) The interaction between an adsorbed molecule and the sieve is characterized by the Henry's law constant which may be determined experimentally

from the limiting slope of the single-component isotherm at low concentrations.

With these assumptions the average number of molecules per cavity is given by

$$\bar{c} = \frac{Kf + \sum_{n=2}^m \left[\frac{(Kf)^n \left(1 - \frac{nb}{v'}\right)^n}{(n-1)!} \right]}{1 + Kf + \sum_{n=2}^m \left[\frac{(Kf)^n \left(1 - \frac{nb}{v'}\right)^n}{n!} \right]} \quad (7)$$

where m is the saturation limit (an integer) determined by the condition $m \leq v'/b$. The advantage of this model is that with only a few parameters (K , b , v') pure component sorption data can be predicted. The α cage volume, v' , is a constant for a specific zeolite and has units of \AA^3 . The Henry's law constant can be determined from the limiting slope and is expressed in terms of molecules/cavity·torr. The effective sorbate molecular volume, b , can be determined by choosing a value for b such that the data fits the model. The effective sorbate molecular volume can be expressed in terms of \AA^3 per molecule. The fugacity, f , is determined using generalized virial coefficients. The amount adsorbed can be expressed in terms of mmoles per gram adsorbent by using the conversion factor 0.56 mmoles/gm per molecules/cavity as suggested by Ruthven (6).

SYSTEM SELECTION

There are three types of methods commonly used to determine equilibrium isotherms for the adsorption of gases in zeolites. Two types are indirect, while the third is a direct measurement. One of the indirect methods often encountered utilizes a breakthrough curve for a packed column, which can be analyzed to obtain the isotherm. The other indirect method makes use of chromatographic data to obtain the isotherm. Direct measurements are made using either volumetric or gravimetric methods.

The gravimetric method was chosen for this work because it is generally subject to less error than the indirect methods. A comparison of the gravimetric method with the volumetric method indicates that the response speed, and accuracy give the gravimetric method the advantage. Another factor in favor of the gravimetric method is its ability to pick up the presence of impurities such as moisture. To obtain data that is reproducible, the sieve must be completely regenerated before measurement of an isotherm. This is checked with the electrobalance by simply obtaining a constant weight on the recorder (4). An advantage that is of

importance to the user is that there are no dead volumes or doser volumes to calibrate with helium or mercury. Also, there are no McLeod gauges or manometers to contaminate the system with mercury or oil (19).

The sorbent chosen for the system was 5A molecular sieve. Linde 5A molecular sieve was chosen as the sorbent because only physical adsorption of methane on sieve occurs. There is no hysteresis. For these reasons and because of the fact that 5A sieve has such a high affinity for impurities, it is reasonable to assume that an apparatus capable of measuring accurate adsorption isotherms on 5A sieve will probably be able to do so for spent or raw shale sorbents.

Molecular sieves belong to a class of compounds known as zeolites. The crystal structure of zeolites has been explained in detail by Breck (20). There are both natural and synthetic zeolites. Synthetic zeolites were produced because the scarcity and high degree of chemical and physical variability made the use of natural zeolites in commercial separation processes impractical.

Synthetic molecular sieves are crystalline zeolites having a basic formula of $M_{2/n}O \cdot Al_2O_3 \cdot xSiO_2 \cdot yH_2O$ where M is a cation of n valence. The fundamental building-block of the molecular sieve crystal structure is a tetrahedron of four oxygen anions surrounding a smaller silicon or aluminum cation. Calcium ions or other cations serve to

make up the positive charge deficit in the alumina tetrahedra. Each of the four oxygen anions is shared, in turn, with another silica or alumina tetrahedron to extend the crystal lattice in three dimensions.

The resulting crystal is honeycombed with relatively large cavities. Each cavity is connected with six adjacent ones through apertures or pores. These cavities are known as α cavities. An α cavity has a free diameter of approximately 11.4 \AA and a volume of 776 \AA^3 . Type 5A has a free aperture size of 4.2 angstroms. Molecules up to 0.5 angstroms larger than the free diameter of the aperture can easily pass through due to the elasticity and kinetic energy of the molecules coming in. Molecules that can pass through the aperture are for example, H_2O , NH_3 , H_2S , CO_2 , SO_2 , and the normal paraffins, C_3H_8 through $\text{C}_{22}\text{H}_{46}$.

Molecular sieves retain adsorbates by strong physical forces rather than by chemisorption. This means that the chemical state of the crystal does not change. It is the same when the adsorbed molecule is desorbed by the application of heat or displacement with another material as when the molecule entered. This indicates that there should be no hysteresis. The adsorption and desorption are completely reversible and their respective curves identical.

Molecular sieve will also adsorb selectively based on polarity or degree of saturation. The less volatile, the more polar or the more unsaturated a molecule the more tightly it is held within the crystal. This is due to the cations in the crystal lattice, sites of strong localized positive charge, which attract the negative end of polar molecules. Unsaturated molecules can have dipoles induced in them under the influence of the strong positive charge of the cations (21).

Isotherms were determined on three forms of Linde 5A sieve. Two forms contain approximately twenty percent clay binder and were obtained as 1/16th inch pellets and 100-120 mesh powder. The pellets (Lot Number 5943350231) were provided by Union Carbide. The powder (Stock No. 5632) was provided by Altech Associates. Dr. Ruthven supplied the pure sieve crystals (Lot Number 560010) which he obtained from Union Carbide.

Methane was chosen as the sorbate over other n-paraffins because its critical temperature is 190.6°K compared with 305.4 and 369.8°K for ethane and propane, respectively. In the higher pressure region that will be examined methane will not condense.

The gas used was 99.97 percent ultra high purity methane obtained from Union Carbide. The possible contaminants were CO_2 , O_2 , N_2 , C_2H_6 , C_3H_8 , and H_2O .

EXPERIMENTAL DESIGN

Three experimental parameters must be measured and controlled in determining an equilibrium isotherm. They are temperature, pressure and weight change. Figures 1 and 2 are schematic diagrams of the apparatus and control panel required.

Most gravimetric adsorption equipment using microbalances is limited to atmospheric pressure and below because most electrobalances are housed in glass. So this study could be conducted at pressures as high as 100 psia, it was necessary to design a special vessel to house the balance.

The actual vessel design was a modification of a design used by Conoco (22). The vessel is shown in Figure 3. It is of stainless steel construction throughout. The two flanges are held in place by twelve brass bolts. Two hangdown tubes are required; one for the sample hangdown ribbon and one for the counterweight hangdown ribbon. Swagelok male connectors were used to connect the tubing to the female pipe ports. Two ports for the electrical feedthroughs were needed because there were fourteen electrical connections

SYMBOL INDEX FOR FIGURE 1

A	Bellows vacuum valve - 1/4"
B	Bellows vacuum valve - 1/2"
C	Bellows vacuum valve - 1/4"
D	Needle valve - 1/4"
E	Bellows vacuum valve - 1/4"
F	Needle valve - 1/4"
G1	Adjustable relief valve - 1/4"
BF	Bath or furnace
CU	Balance control unit
DP	Diffusion Pump
HT	Hangdown tube
HVG	High vacuum gauge
LNT	Liquid nitrogen trap
RC	Recorder
RP	Roughing pump
ST	Sieve water trap
TR	0-250 psia transducer
WT	Wallace and Tiernan gauge
1	Thermistor gauge 1
2	Thermistor Gauge 2

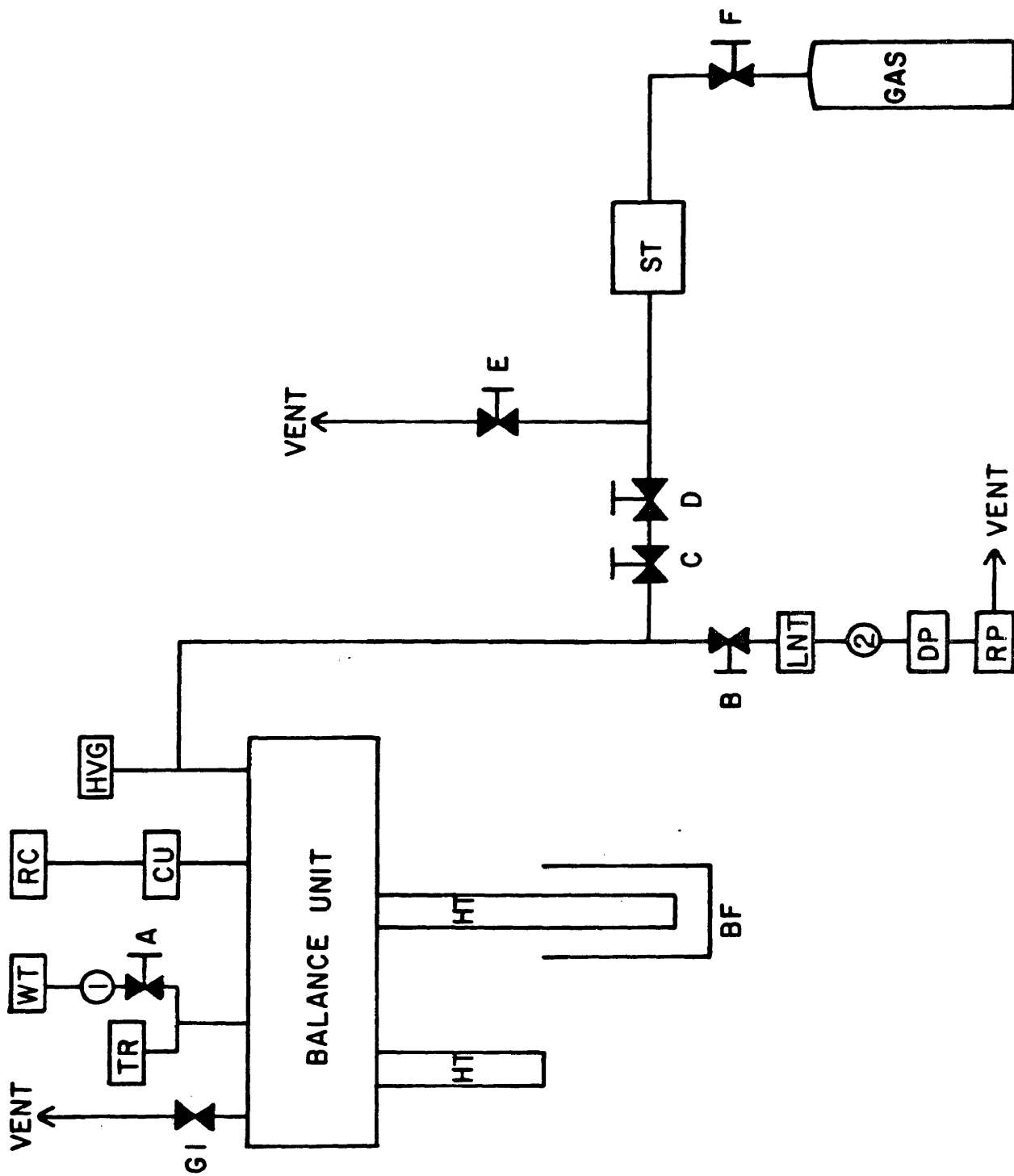


Figure 1. Schematic Diagram of Gravimetric Adsorption Apparatus.

SYMBOL INDEX FOR FIGURE 2

A-E	Valves
CU/	Electrobalance control unit
DPR	Digital Pressure Readout
FL	Warning Light
MECP	Main Electric Control Panel
	a) Warning light
	b) Roughing pump
	c) Diffusion pump
	d) Bath
PTC	Proportional Temperature Controller
RC	Recorder
TG	Thermistor Vacuum Gauges
WT	Wallace and Tiernan Gauge

ARTHUR LAKES LIBRARY
COLORADO SCHOOL of MINES
GOLDEN, COLORADO 80401

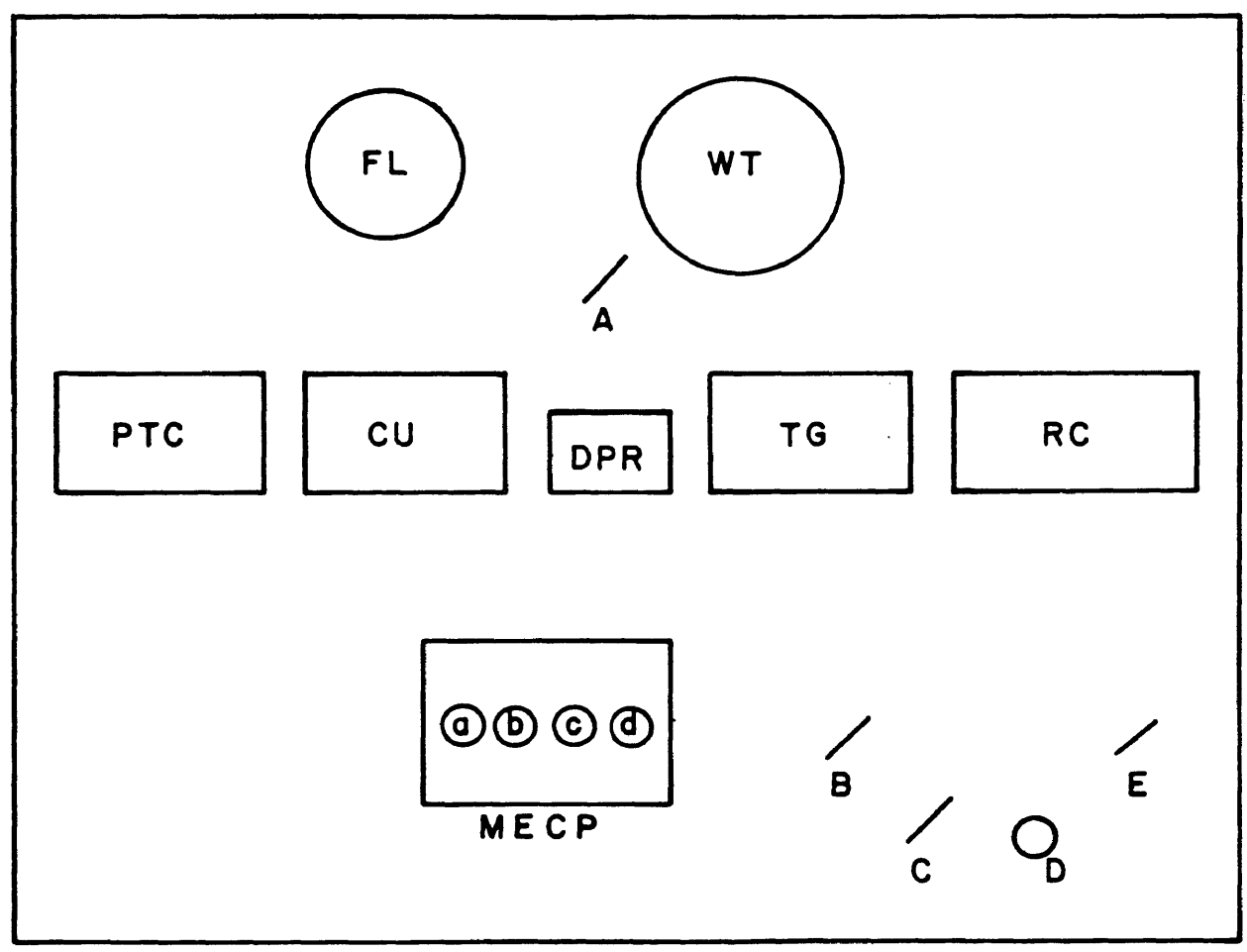


Figure 2. Schematic Diagram of the Control Panel for the Gravimetric Adsorption Apparatus.

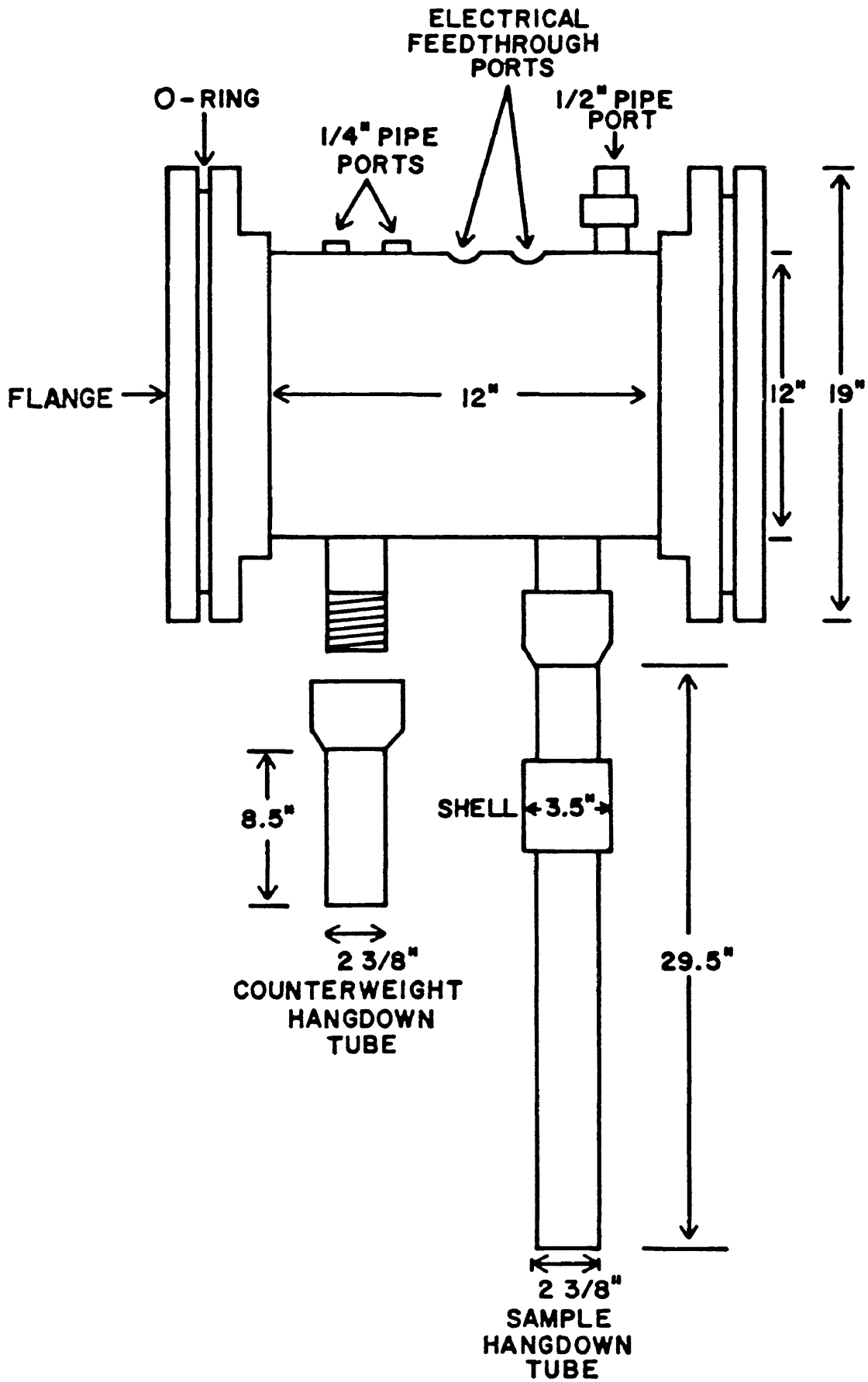


Figure 3. Diagram of Adsorption Vessel.

to the balance and each feedthrough has twelve wires. The sample hangdown tube has a cylindrical shell through which water can flow. This is basically a precaution to assure that the balance doesn't overheat when the sample is regenerated at 400°C. An added safety feature is the adjustable in-line relief valve, which is set to open if the pressure exceeds 150 psia.

The Cahn Model R-100 Electrobalance is basically an electric current-to-torque transducer. The major components of the electrobalance are shown in Figure 4. The electrobalance consists of: (1) a balance beam that pivots around the center of a taut ribbon; (2) a torque motor coil in a permanent magnetic field; (3) hangdown ribbons for the sample and counterweights; (4) a beam position sensor system consisting of a light source, flag, light tubes, and photodiode, and (5) the control unit. The balance unit is usually housed in a glass bell jar for vacuum work. This bell jar was removed because of the balance's sensitivity to static electricity. Since the balance unit is confined to the stainless steel vessel, two pairs of electrical connectors were required. One inside the vessel to connect the balance unit to the electrical feedthrough and one outside the vessel to connect the feedthrough to the control unit. So that the balance temperature could be monitored on a recorder a Type T copper-constantan thermocouple was attached to thermocouple location 2 in Figure 5.

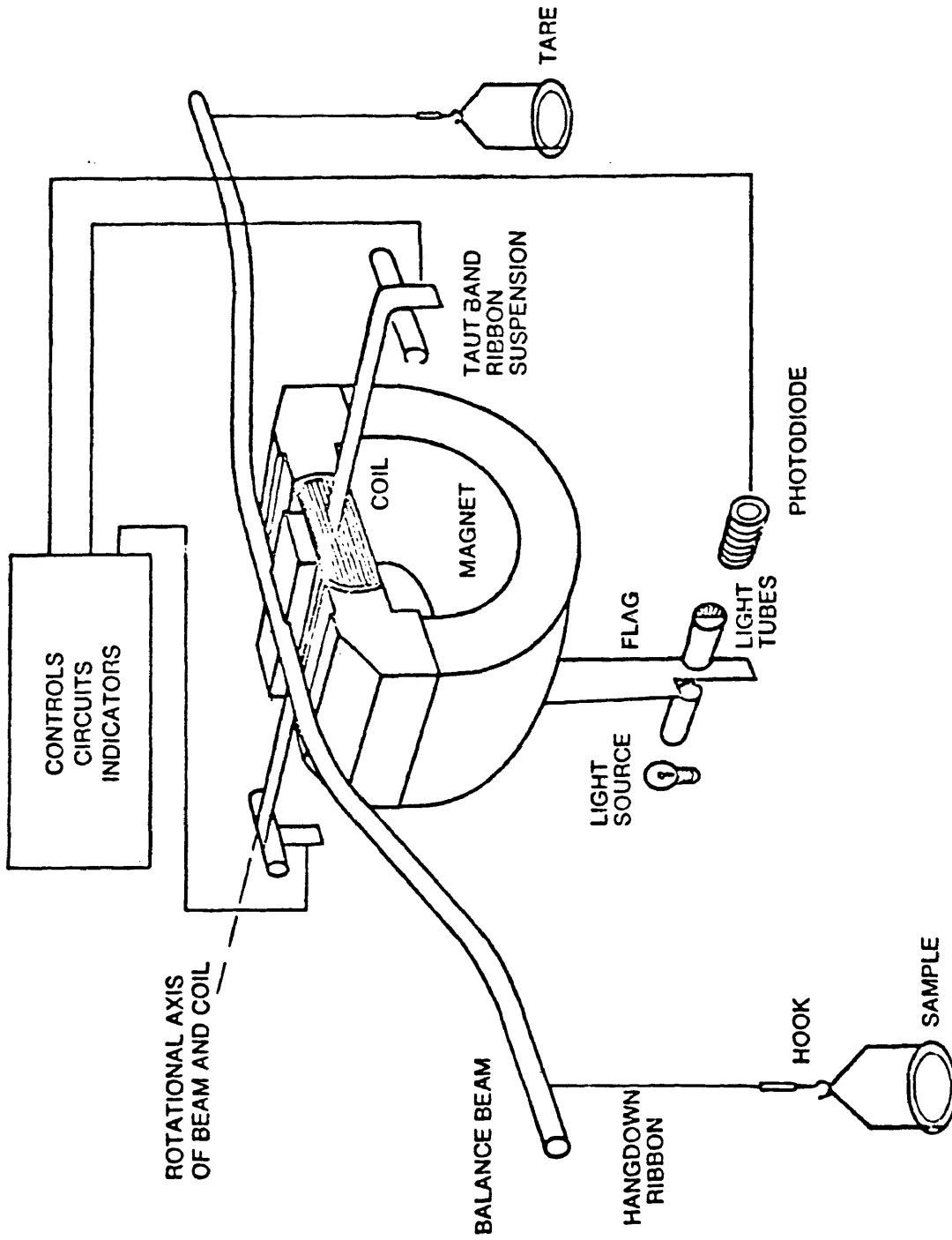
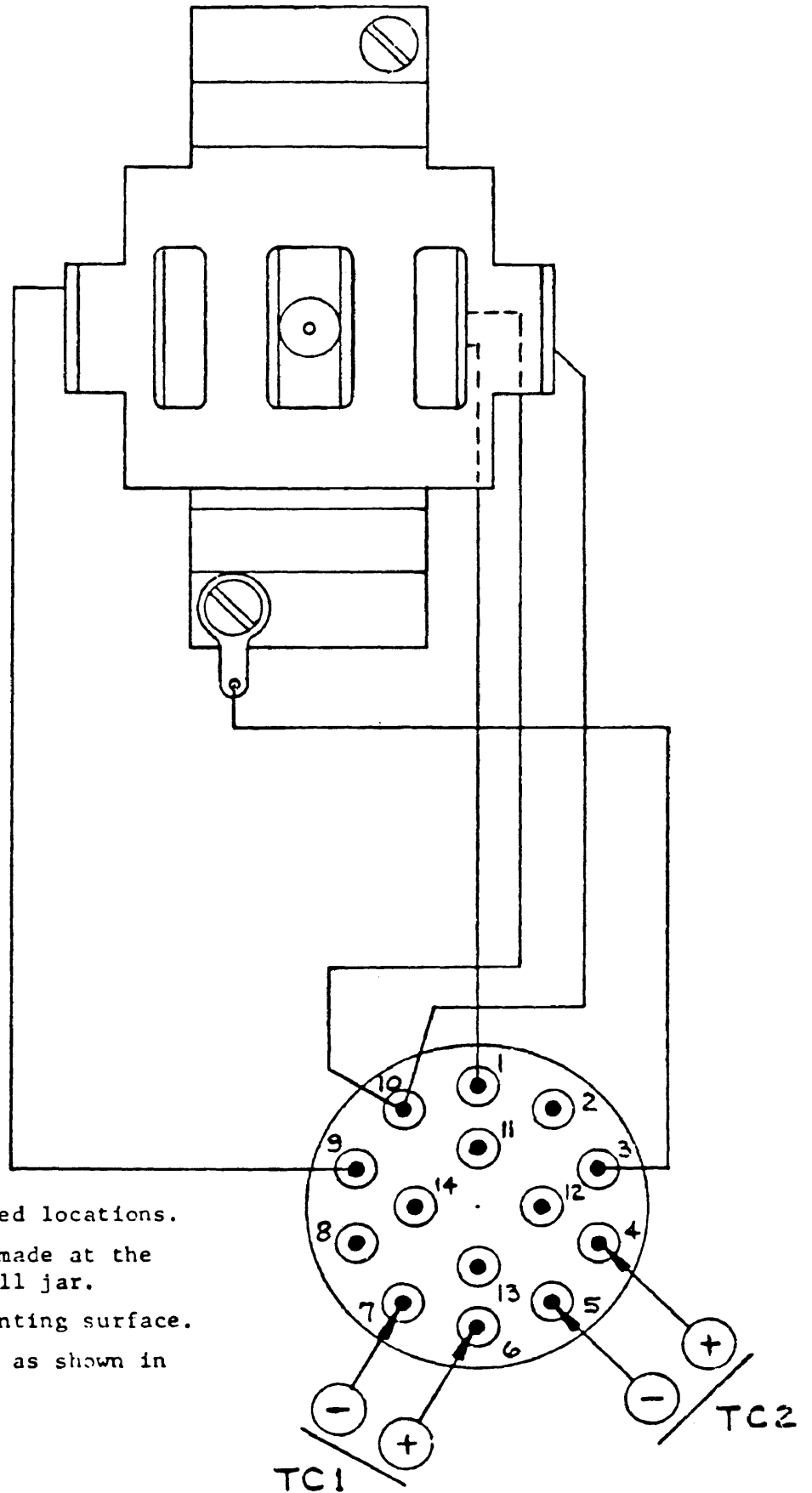


Figure 4. Diagram of Cahn Model R-100 Electrobalance



1. Locate thermocouples at desired locations.
2. Thermocouple connections are made at the 14 pin connector under the bell jar.
3. Pin #1 is facing the rear mounting surface.
4. Connect thermocouples to pins as shown in diagram.

Figure 5. Cahn Model R-100 Electrobalance Thermocouple Connection Diagram.

The electrobalance should have a maximum sample capacity of 100 grams, a sensitivity of 0.5 micrograms and a temperature stability of less than or equal to $10 \mu\text{g}/^\circ\text{C}$ between 20 and 25°C when the beam is fully tared. The temperature stability is substantially less when carrying a 100 gram load with maximum electrical suppression. In this case it should be less than or equal to $150 \mu\text{g}/^\circ\text{C}$.

The sample weight and electrobalance temperature were recorded on a Moseley Model 7100B Strip Chart Recorder. This model has two independent pen drives and accomodates two input modules. The chart speed ranges from 1 inch per hour to 2 inches per second.

The vacuum system was assembled to fit the vacuum requirements of the apparatus with the help of Mr. Gene Witney of Remanufactured Vacuum Products. The roughing pump is a two-stage Welch Duo-Seal Vacuum Pump. The free air displacement is 60 liters per minute with a guaranteed pressure of 0.1 microns at the pump inlet. The diffusion pump is water cooled and requires approximately 70 cc of Dow Corning 704 diffusion pump fluid. A liquid nitrogen cold trap was added to prevent back diffusion of the pump fluid during regeneration of the sample. This trap is a three-foot U-shaped section of half-inch copper tubing around which a dewar flask containing liquid nitrogen can be raised when required.

Temperature control around the sample hangdown tube was maintained using a refrigerated/heated bath and circulator. The temperature range of the bath is -20°C to 70°C . Precise control can be provided to within 0.1°C . External circulation was used with the aid of copper tubing and a dewar flask. Copper tubing, 1/4 inch in diameter, was wrapped around the hangdown tube and the flask raised into position. For runs at room temperature tap water was used in both the bath and the dewar. For isotherm temperatures less than or equal to 0°C a mixture of tap water and anti-freeze was required. Temperatures were measured using a Tagliabue thermometer.

During the regeneration procedure a Forma tubular heater was raised around the hangdown tube. The proportional temperature controller is a part of the control panel, but was not used because sufficient temperature control was achieved using a Variac. Glass wool was packed around the top of the furnace to prevent convection heat losses. Since these temperature measurements need not have been very accurate a simple Honeywell Temperature Indicator with a Type K thermocouple was used. The circulating bath was connected to the cylindrical shell on the sample hangdown tube and controlled at 10°C to keep the balance from overheating.

Pressure measurement at high vacuum conditions was achieved using the Discharge Vacuum Gauge, Type GPH-100A.

This gauge does not appear on the control panel layout because it is located on the shelf on the left side of the control panel. It has three scales ranging from 10^{-7} to 25×10^{-3} torr. In the region where maximum vacuum for the apparatus was obtained the meter could be accurately read to 0.0001 torr.

Pressure in the region from 1 to 800 torr was measured with a Wallace and Tierman Absolute Pressure Gauge. This gauge has an accuracy of 0.5 torr and has 1.0 torr graduations. If this gauge should become damaged or lose accuracy, there is a backup 0 to 25 psia transducer with digital pressure readout available for use. The estimated accuracy of the transducer is roughly one torr. The pressure region from 800 torr to 100 psia was measured using the 0 to 250 psia transducer with digital pressure readout. The estimated accuracy in this region is 0.1 psia or 5 torr. The wiring diagram for the transducers is shown in Figure 6.

The thermistor gauges measure the pressure at two different locations in the system when the vacuum pump is in operation. Thermistor Gauge 1 is placed directly above the diffusion pump because the diffusion pump should not be switched on until the pressure at this point is at least 50 microns. Thermistor Gauge 2 monitors the system pressure in the region between 25 microns and 1 torr.

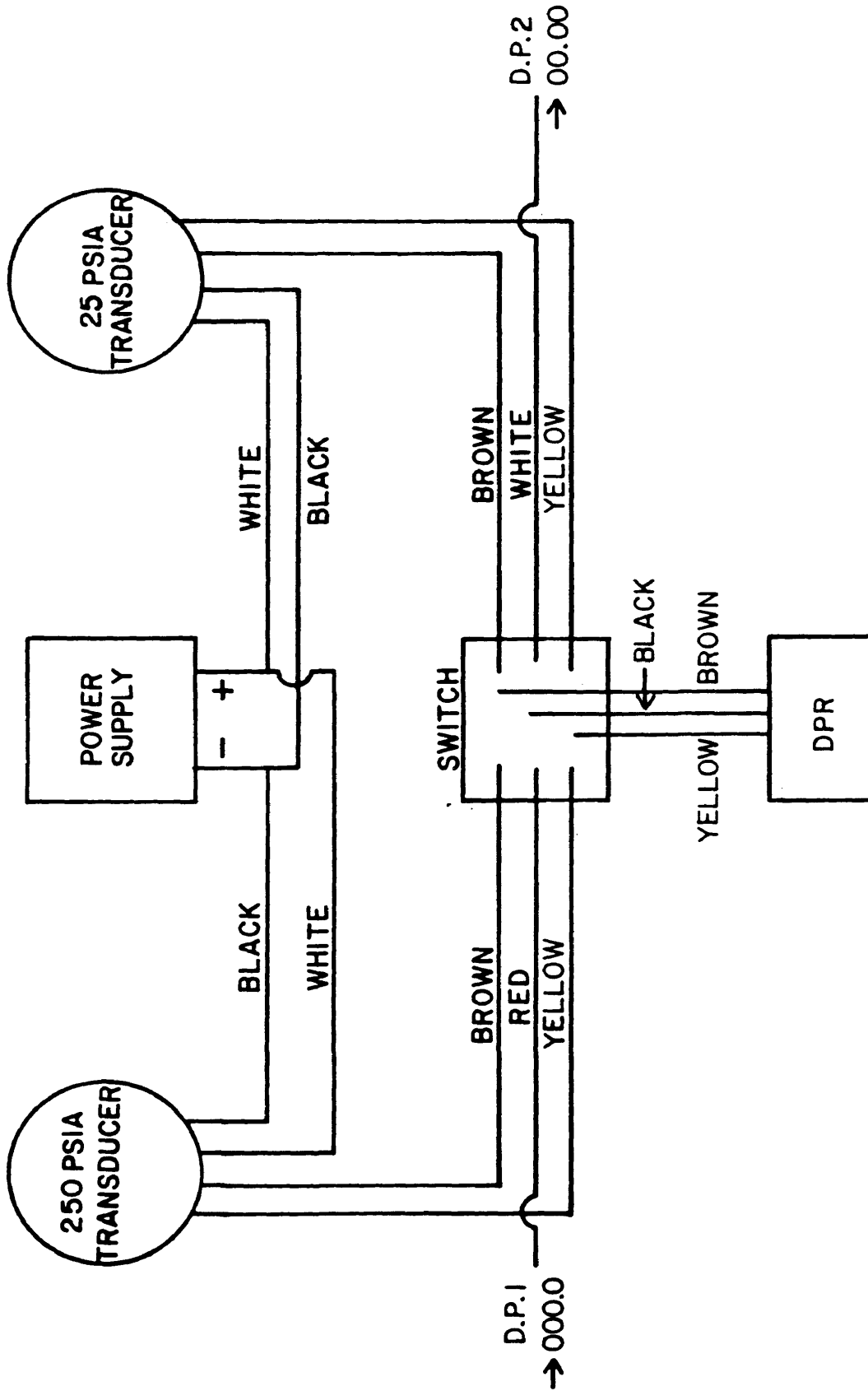


Figure 6. Wiring Diagram for the Pressure Transducers.

The water trap was included in the system because 5A molecular sieve has a high affinity for water vapor. Previous investigators (4) found that a water trap of some type was required even when the adsorbate was 99.96 percent pure methane. Since there were plenty of 4A zeolite pellets on hand, these pellets were packed into a ten-foot coiled copper column with a diameter of approximately 1/2 inch. The sieve in the column was heated with heating tapes and evacuated during the regeneration procedure to minimize any chance that it might become saturated with water from the methane gas.

SYSTEM CALIBRATION AND PERFORMANCE

The electrobalance, itself, does not require calibration because this operation is performed in the factory prior to shipment. However, the output of the balance must be in agreement with the recorder. To calibrate the recorder a 100 milligram Class M weight is placed on the sample pan with the meter and recorder range set at 100 milligrams. The recorder calibrate knob at the rear of the electrobalance control unit was adjusted until the recorder read 100 percent. Calibration was also checked with Class M weights.

The balance performance was acceptable except for a problem encountered with temperature drift. The manual specifies a maximum drift of 10 $\mu\text{g}/^\circ\text{C}$. Figure 7 shows the weight deviation with room temperature. It was determined that both the control unit and balance unit were temperature sensitive, though the balance unit showed the most temperature sensitivity. The actual temperature drift is approximately 27 $\mu\text{g}/^\circ\text{C}$. A Cahn representative suggested that a potentiometer in the control unit be adjusted. This was done, but did not alleviate the temperature drift. Rather than return the balance to Cahn, an effort was made to keep

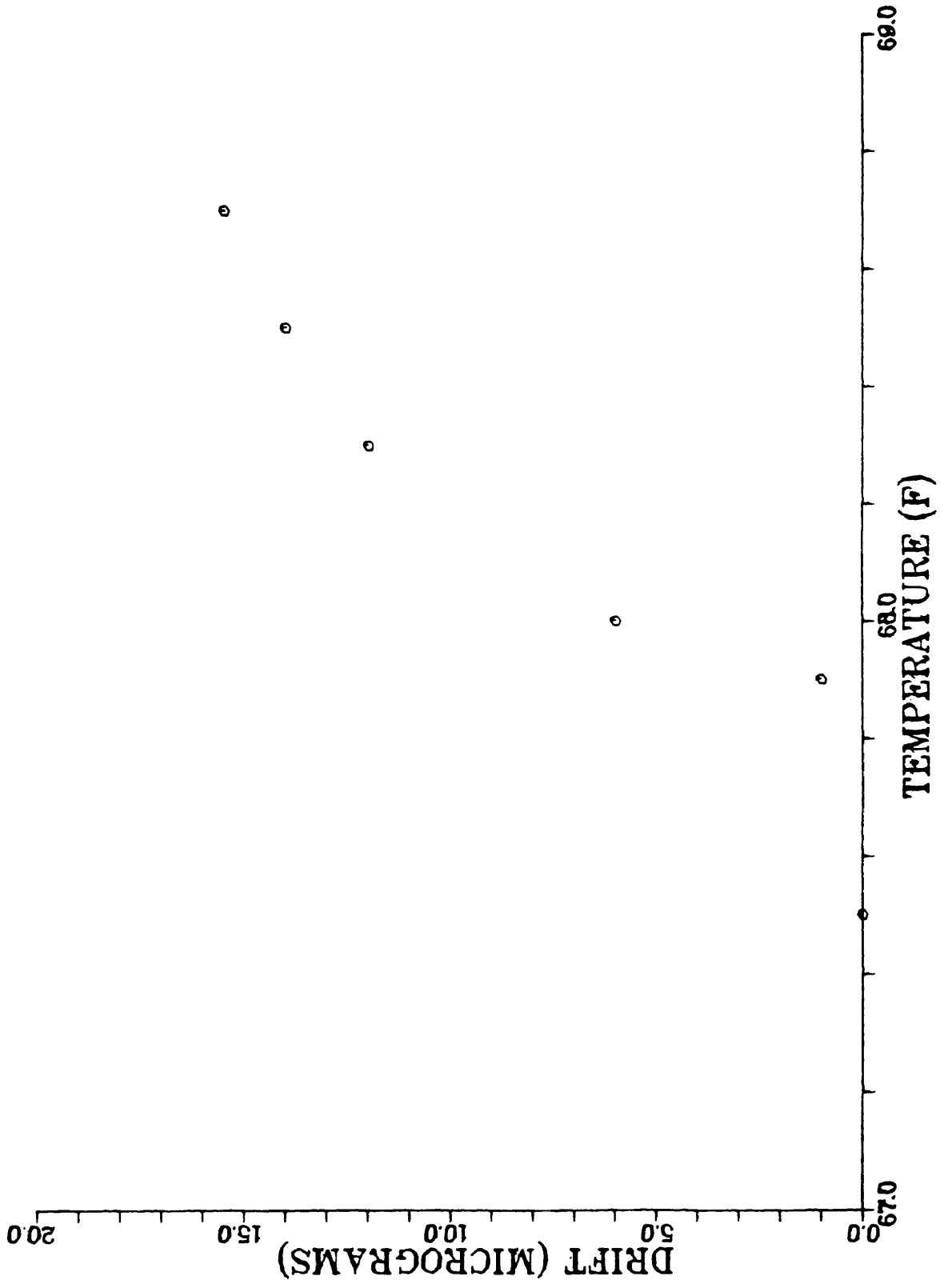


Figure 7. Weight Drift with Temperature.

the room temperature as constant as possible by covering the windows with aluminum foil and adjusting the room thermostat. The room temperature during a run was controlled to within $\pm 1.0^\circ\text{F}$ of the temperature at which the balance was zeroed.

The calibration report for the Wallace and Tiernan gauge is traceable to the National Bureau of Standards. As a check, the gauge was exposed to atmospheric pressure. The gauge indicated 622.3 torr and the barometer indicated 622.2 torr. Calibration curves for the transducers using both the manometer and a dead weight tester are given in Figures 8-10. The calibration for the vacuum gauges was conducted by Ball Brothers Research Corporation in Boulder, Colorado.

A vacuum of 6.5×10^{-4} torr was achieved with a leak up rate of approximately 8×10^{-3} torr per hour. This leakage was probably due to a combination of actual and virtual leaks. Better vacuums have been achieved by other investigators. Some on the order of 10^{-6} torr were achieved, but their systems were designed to measure isotherms below atmospheric pressure. Compression fittings were required for this apparatus and though a semi-rigid epoxy was applied to these fittings the vacuum did not improve much. The conductance of the 1/2 inch and 1/4 inch tubing also does not favor high vacuum.

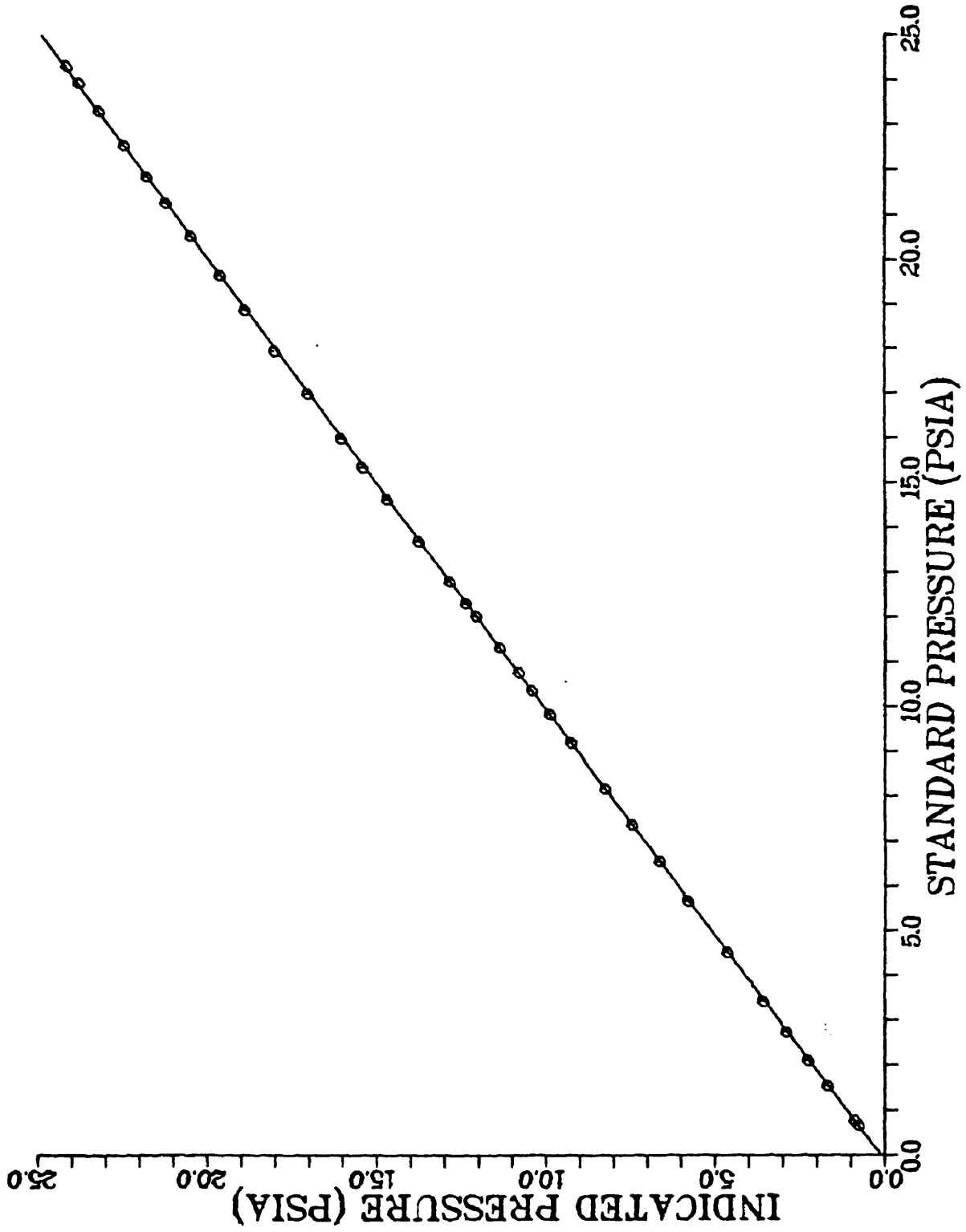


Figure 8. Calibration Curve for 25 psia Transducer Using Mercury Manometer.

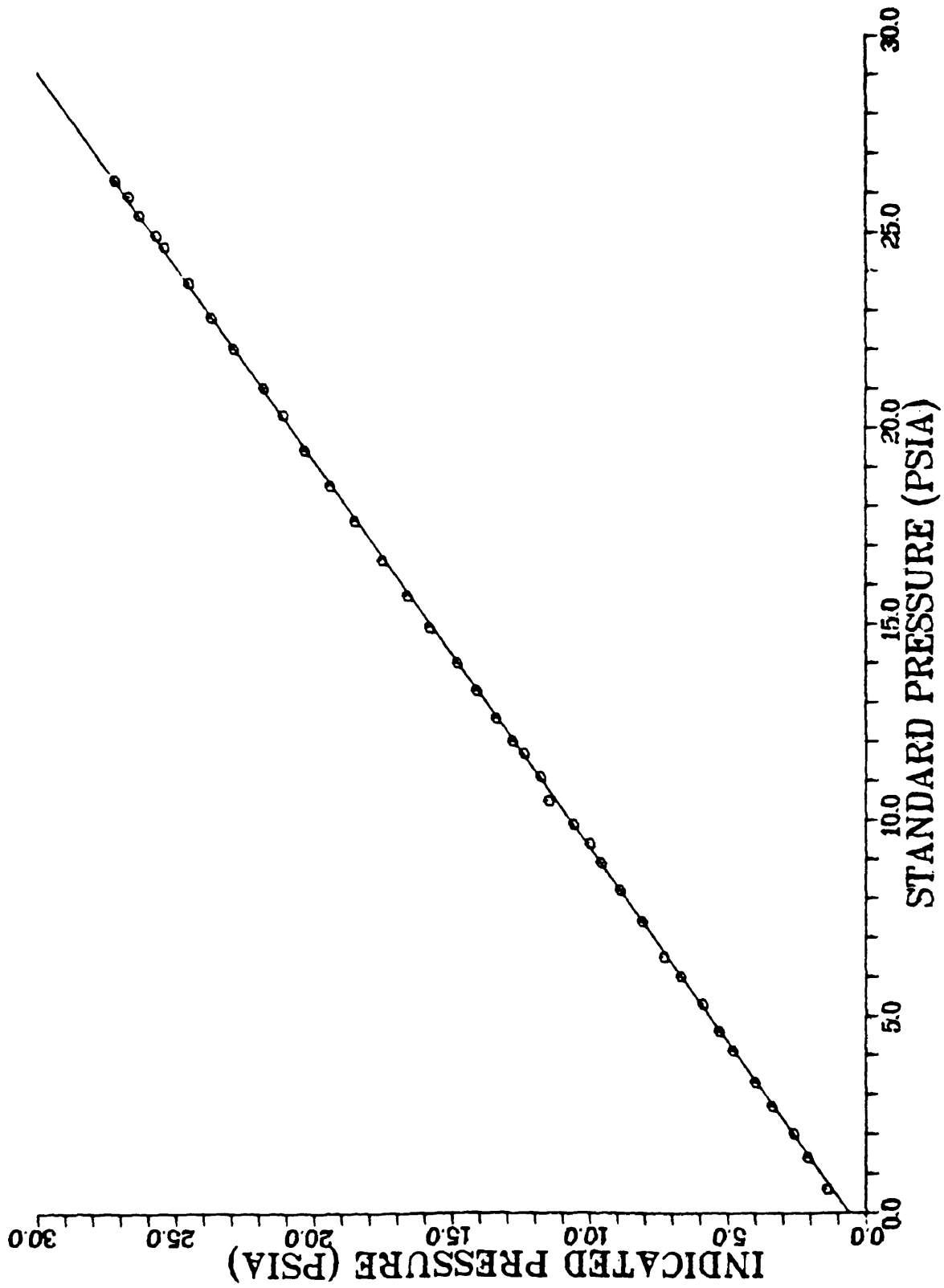


Figure 9. Calibration Curve for 250 psia Transducer Using Mercury Manometer.

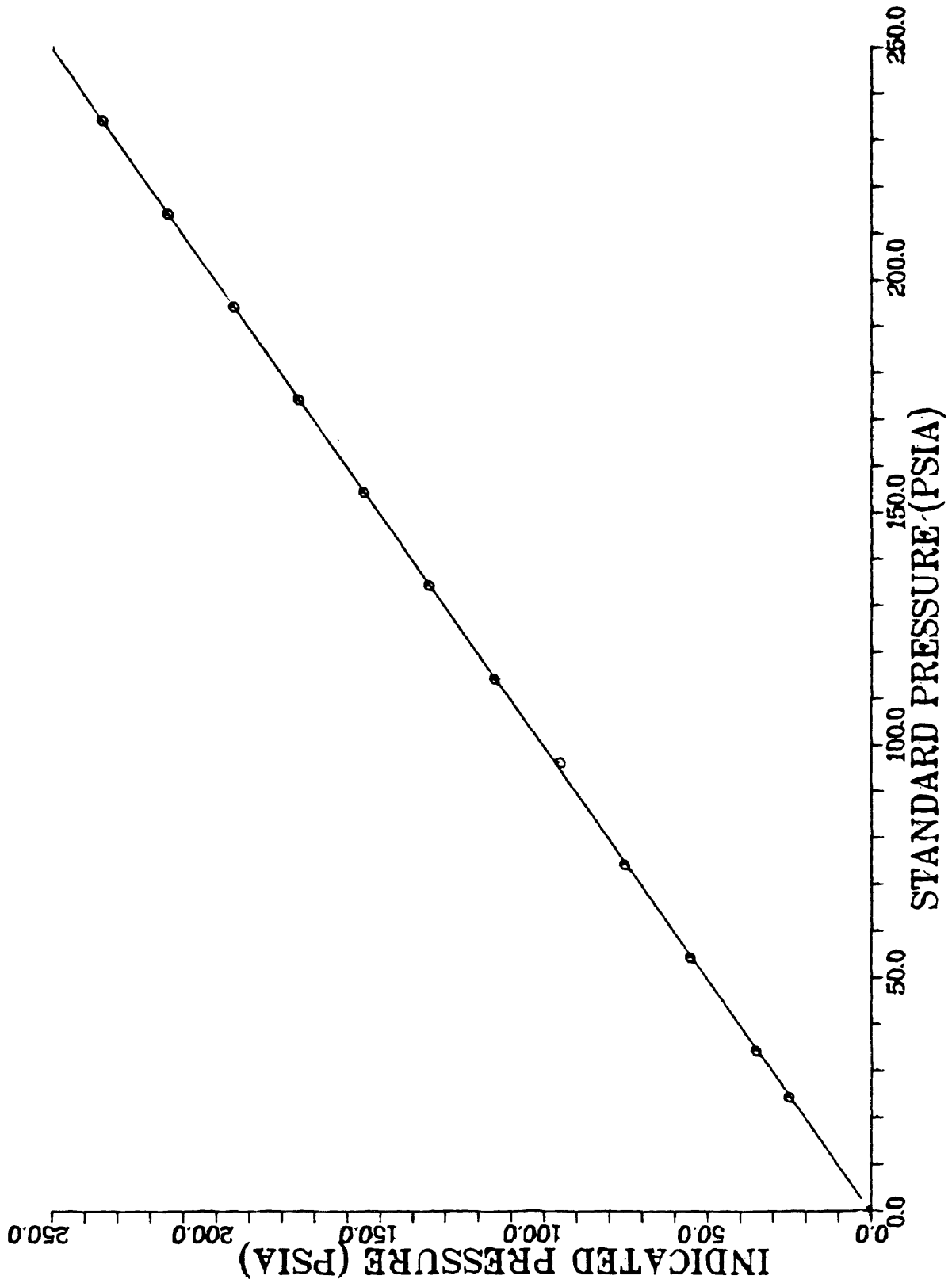


Figure 10. Calibration Curve for 250 psia Transducer Using Dead Weight Tester

Pressure tests were also conducted. These results are shown in Table 1. The "Predicted Pressure" was obtained using the ideal gas law. Helium was the gas used to conduct this test.

The equilibrium temperature was measured using Tagliabue thermometers numbers 757866 and 757556. These thermometers are certified and their calibration is traceable to the National Bureau of Standards.

Table 1

Pressure Leak Test

<u>Date</u>	<u>Time</u>	<u>Temperature (°F)</u>	<u>Pressure (psia)</u>	<u>Predicted Pressure (psia)</u>
4-6-77	10:30 a.m.	69	146.7	147.0
	12:00	70	147.0	147.5
	1:00 p.m.	72	147.4	148.5
	3:00 p.m.	76	148.3	149.1
	5:00 p.m.	79	149.1	
4-7-77	9:00 a.m.	71	147.7	147.3
	12:30 p.m.	74	148.1	147.9

EXPERIMENTAL PROCEDURE

This section describes the experimental procedure used in operating the equipment. All references are made with regard to Figure 1. Future operators may need to modify this procedure for their own use. These modifications will be minor in that they will most likely involve regeneration time and regeneration temperature.

The balance was zeroed prior to each adsorption run. The zeroing procedure is described in Cahn Instruments Instruction Manual #5005. Make sure that the zeroing procedure and all weight determinations are conducted with the hangdown tubes in place.

Regeneration of Adsorbent

- 1) The load should be tared if the sample size is greater than one gram to increase the sensitivity. Weigh counterweight and then transfer to counterweight pan.
- 2) Use the Mettler balance to weigh out the desired amount of sieve and then add to sample pan.
- 3) Close valves E and F.

- 4) Switch vacuum pump on and observe thermistor gauge 2.
It will read off scale to the right for approximately fifteen minutes before coming back on scale.
- 5) Plumb the temperature control bath to the sample hangdown tube and set the bath temperature to 10°C.
- 6) Raise the tubular furnace around the sample hangdown tube.
- 7) Set the temperature indicator thermocouple against the sample hangdown tube and place glass wool around the top of the furnace.
- 8) Raise the liquid nitrogen bath around the trap when thermistor gauge 2 reads 50 microns.
- 9) Make sure water is running through the cooling coils of the diffusion pump.
- 10) Switch diffusion pump on.
- 11) Switch both variacs on.
 - a) Set the sieve trap variac to 60
 - b) Slowly raise the tubular furnace temperature to 150°C and then switch variac off for approximately 10 minutes.
- 12) Slowly increase the temperature to 400°C with the tubular furnace variac.
- 13) Regenerate the sieve to a constant sample weight
(approx. 50 hrs.)

- 14) Regenerate the sieve for about 12 hours on subsequent regenerations following an adsorption run.

Collecting Data

- 1) Switch water trap variac off and wait for trap to cool off.
- 2) Close valve B and lower the temperature to 300°C.
- 3) Preload the sieve by opening valve F and allowing a pressure of 30 or 40 torr to be reached.
- 4) Close valves C and F.
- 5) Remove the furnace after the pressure has equilibrated and put the bath in place.
- 6) Record the sample weight and pressure when temperature equilibrium is reached at the desired temperature.
- 7) Generate points on the adsorption isotherm by opening valves C and F and then closing them when the desired pressure is reached.
- 8) Close valve A and plug in the digital pressure readout when a pressure of 800 torr is reached.
- 9) Open valve E to obtain desorption points above atmospheric pressure.
- 10) Switch the vacuum pump on and open valve B to obtain desorption points below atmospheric pressure.

Vacuum System Shutdown Procedure

- 1) Make sure valve B is closed.
- 2) Remove liquid nitrogen bath and switch off diffusion pump.

- 3) Switch off roughing pump when diffusion pump is cool to the touch.
- 4) Open valve between roughing pump and diffusion pump to bring vacuum system to atmospheric pressure.

Bouyancy Tests

Bouyancy tests were required to determine the effects of the gas on the weight readings other than the effect of actual gas adsorption. A bouyancy test consists of a series of mass measurements at a series of pressures over the pressure range of interest, under conditions identical to those to be used in the actual adsorption experiment. The procedure is exactly like the one used in collecting data, except that glass beads are placed in the sample pan rather than the sorbent. Glass is not a good adsorbent and therefore, any observed weight changes are due primarily to bouyancy. The glass beads have a density of 2.94 grams per cubic centimeter.

The tests were evaluated in a manner similar to that of Sloan (23). The bouyancy correction was determined by examining three contributions to the bouyancy. One was the bouyancy of the sample, which is directly related to the volume of the sample and the density of the gas. The second contribution was the bouyancy of the counterweights. The third accounts for non-linear deviations such as those caused by thermo-molecular flow:

$$b' = m_s \cdot \rho_g / \rho_s - (V_C \cdot \rho_g + C) \quad (8)$$

where

b' = bouyancy, μg
 m_s = mass of sample, μg
 ρ_s = density of sample, $\mu\text{g}/\text{cc}$
 ρ_g = density of gas phase, $\mu\text{g}/\text{cc}$
 V_C = effective volume of counterweight, cc
 C = correction term, μg

The effective counterweight volumes were chosen as those volumes which would give a correction term of zero at 100 psia. These were determined to be 0.714, 0.764, and 0.704 cm^3 for the tests conducted at 273, 298, and 308°K, respectively. Figure 11 shows the data obtained for the bouyancy test conducted at 298°K. This graph suggests that the non-linear effects are small. The maximum value for the non-linear correction term obtained was 19 μgs , which is relatively small compared to the mass adsorbed during an experimental run. The bouyancy tests give values of bouyancy for various gas phase densities, which can be inserted into equation 8 to calculate the correction term at each pressure.

During an experimental run the various values of gas phase density, counterweight volume and correction term are plugged back into equation 8 to determine the bouyancy effect. The bouyancy effect is subtracted from the measured weight change to yield the actual weight change.

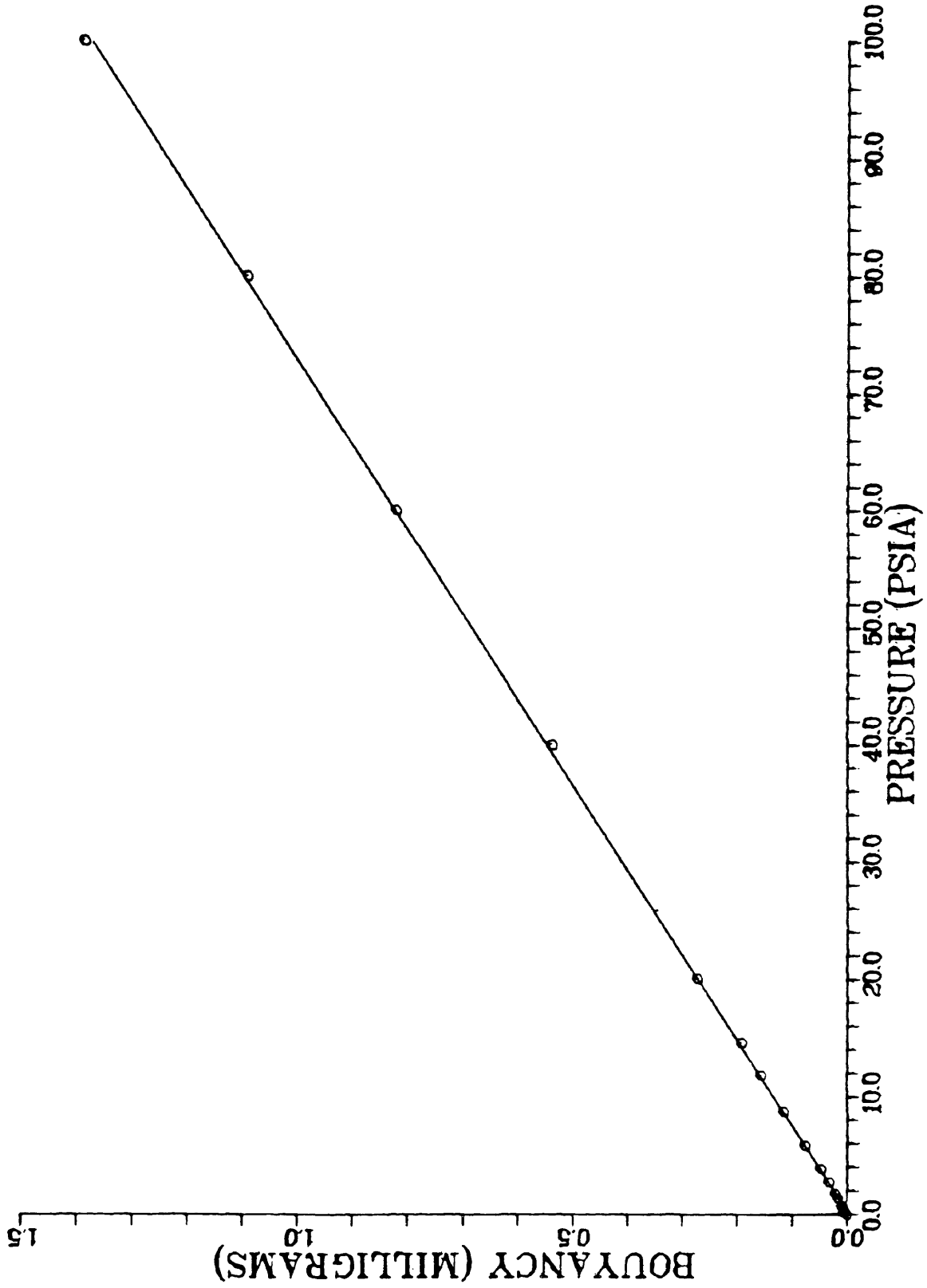


Figure 11. Buoyancy Test Conducted at 298°K.

$$m_a = m_m - b' \quad (9)$$

where b' = bouyancy, μg
 m_a = actual mass, μg
 m_m = measured mass, μg

One difficulty was encountered in conducting the bouyancy tests. Glass does not have the same density as sieve. For the tests to have maximum validity would require that m_s and d_s be kept constant during both the sorption experiments and the bouyancy tests. Since this was not possible, an effort was made to keep m_s/d_s constant. The density of the sieve was found to be 2.20 grams per cubic centimeter.

RESULTS

ARTHUR LAKES LIBRARY
COLORADO SCHOOL of MINES
GOLDEN, COLORADO 80401

The primary goal of this thesis project was to design and construct an experimental apparatus capable of determining accurate adsorption isotherms. Several runs were conducted to test the system.

The methane adsorption isotherms on pure 5A crystals at 273, 298, and 308°K are shown in Figures 12, 13, and 14, based on numerical data given in Tables A1 through A3. The isotherms at 273° and 298°K are then compared with similar data obtained on pellets and powder in Figures 15 and 16 based on numerical data given in Tables A4 and A5.

Isosteres at loadings of 2.0, 4.0, and 6.0 mmoles/g are shown in Figure 17. The variation of isotheric heat of adsorption with loading is given in Table 2. For loading values greater than 0.6 mmoles/g the isosteric heats of adsorption are determined using the 298 and 308°K isotherms, since data was not collected above this loading at 273°K. The isosteric heat of adsorption of methane derived from the isotherm data was found to be approximately 5.0 Kcal/mole.

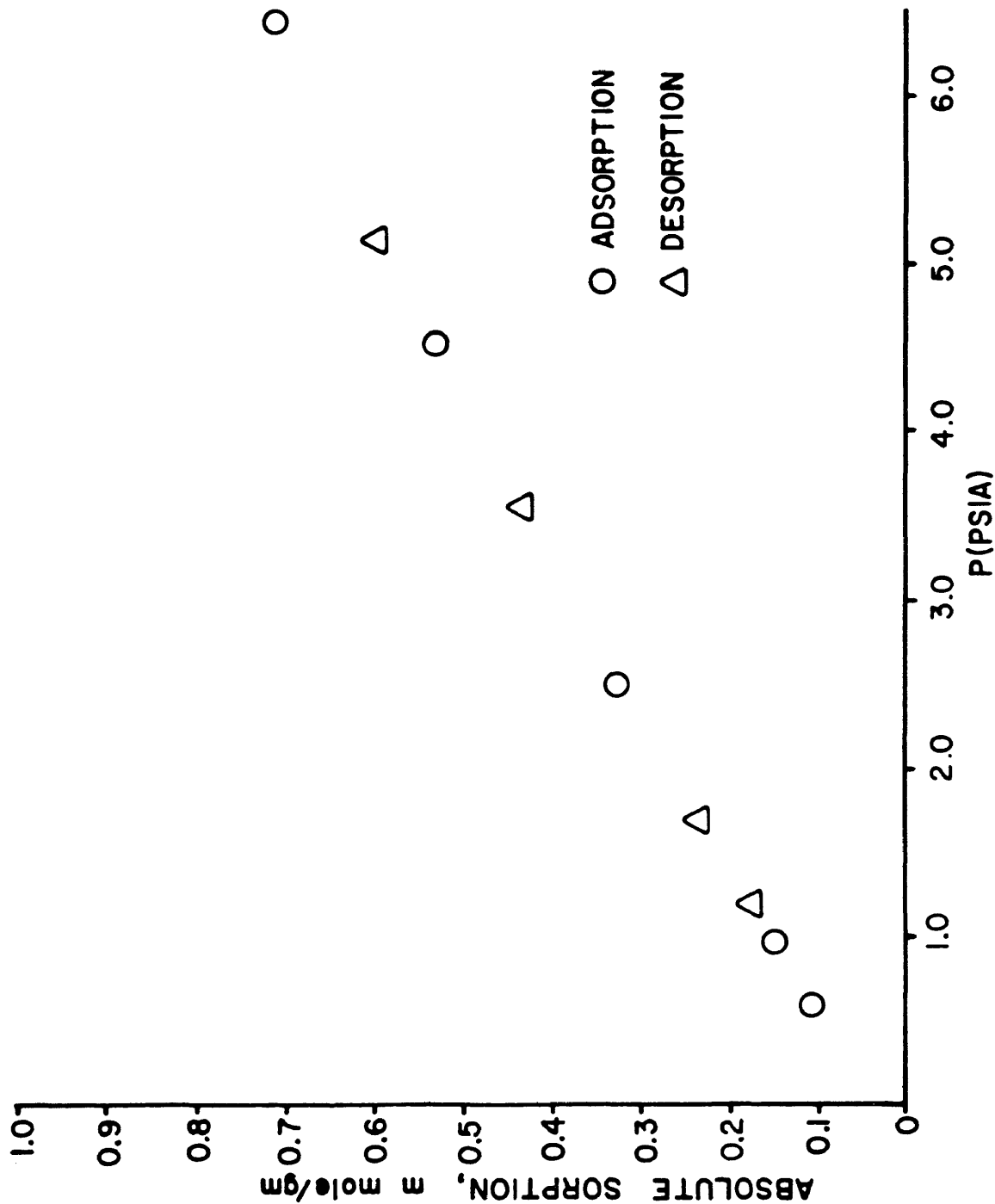


Figure 12. Adsorption Isotherm for Methane on 5A Crystals at 273°K.

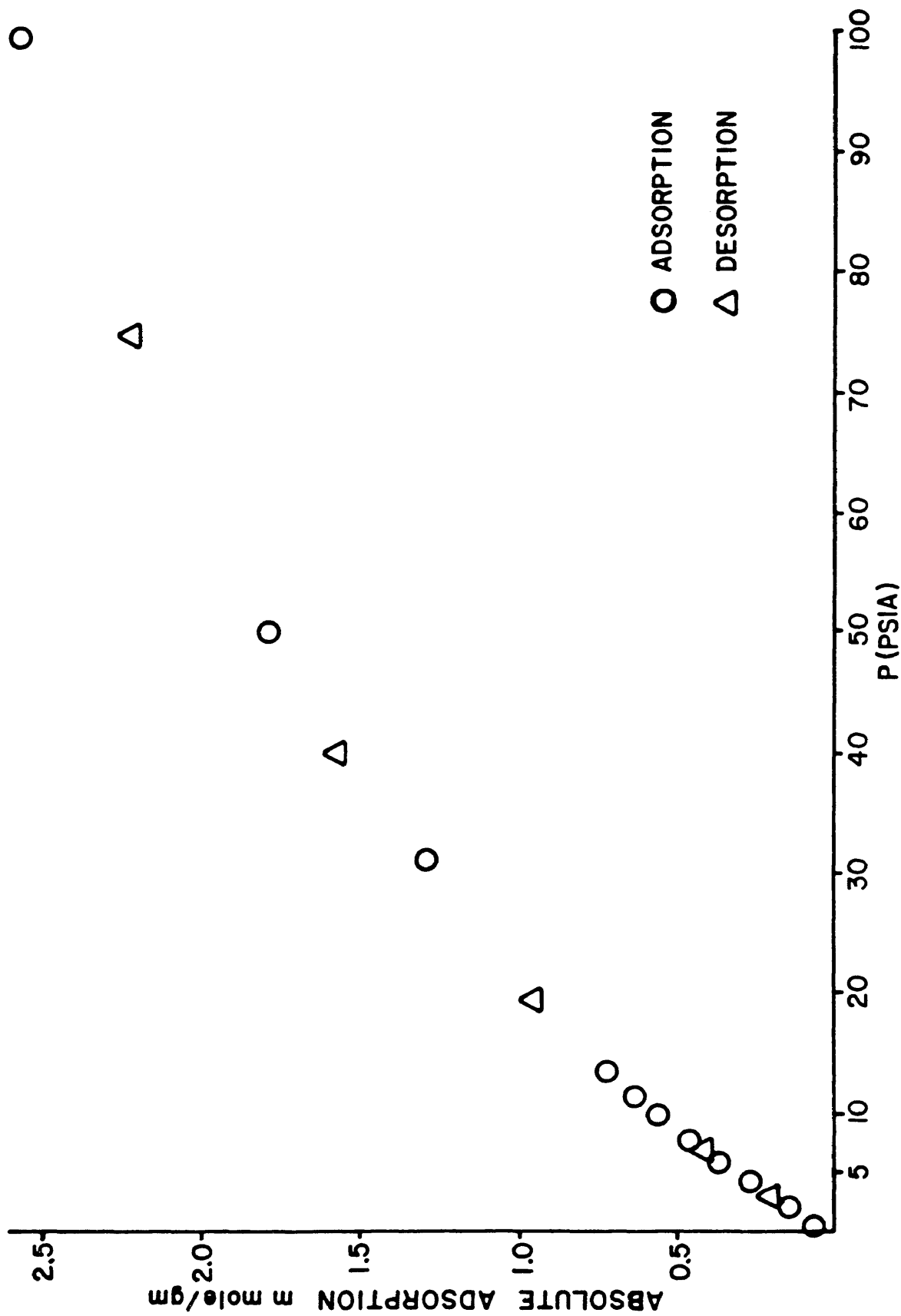


Figure 13. Adsorption Isotherm for Methane on 5A Crystals at 298°K.

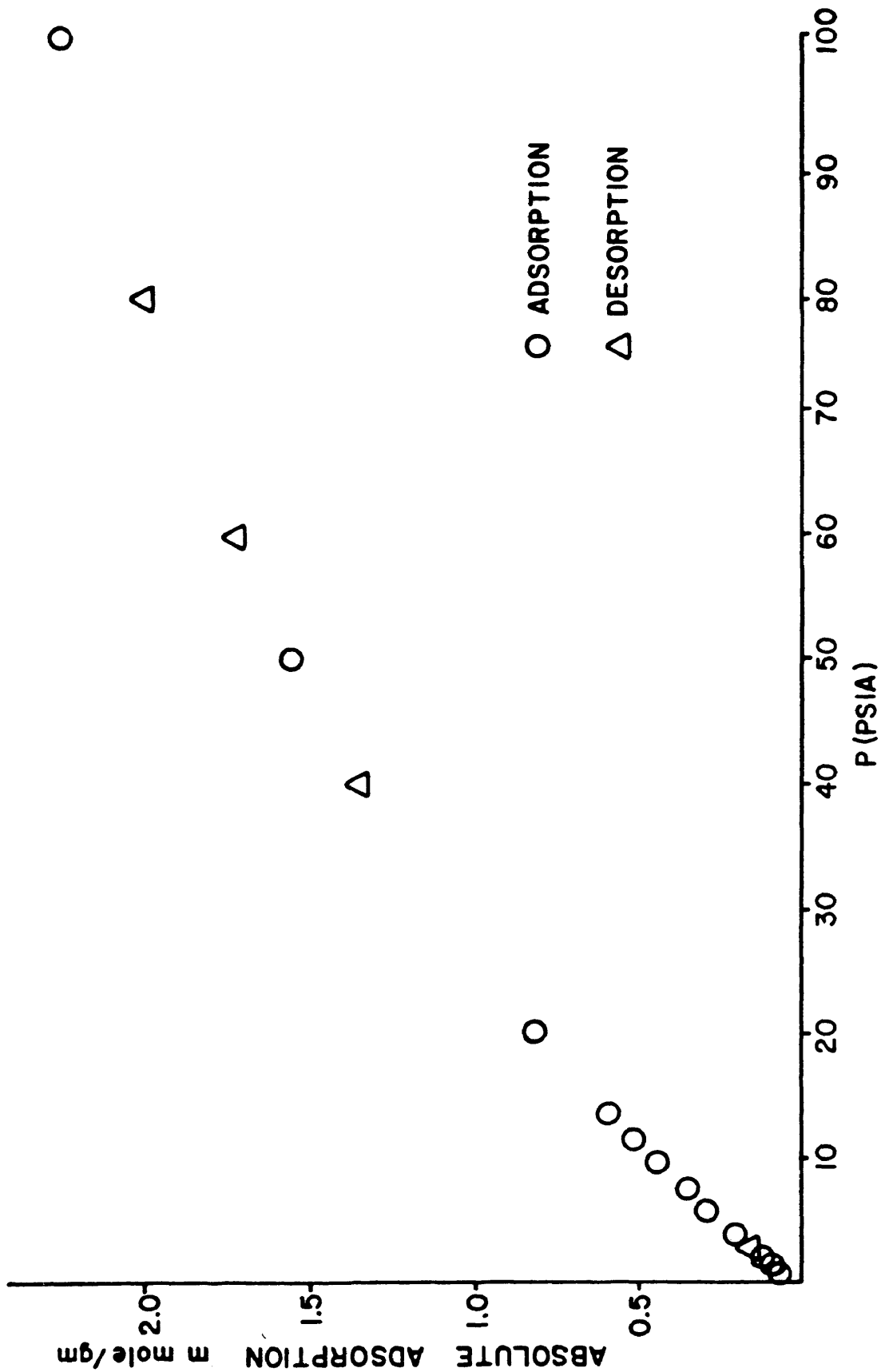


Figure 14. Adsorption Isotherm for Methane on 5A Crystals at 308°K.

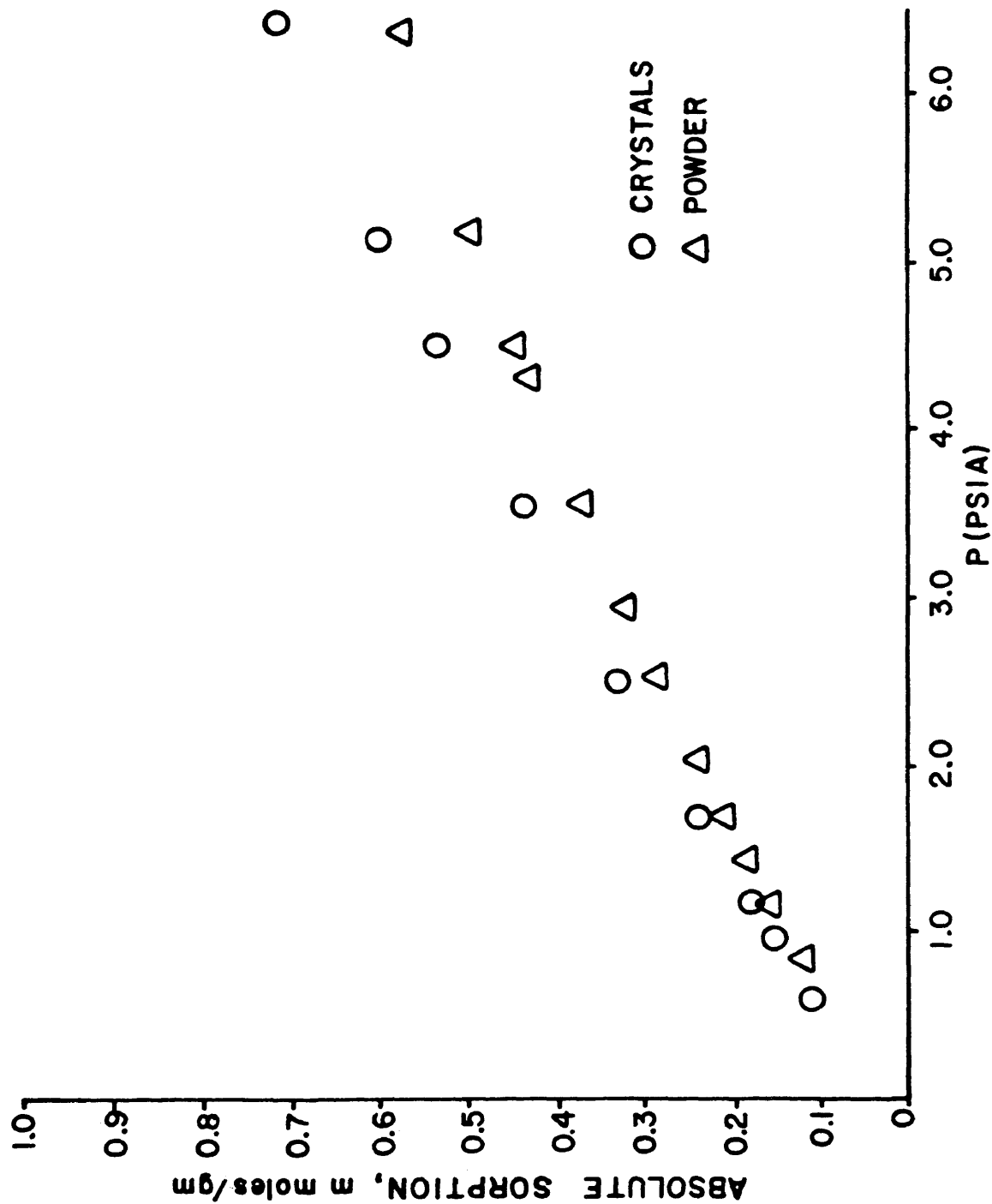


Figure 15. Comparison of Methane Adsorption Isotherms on 5A Crystals and Powder at 273°K.

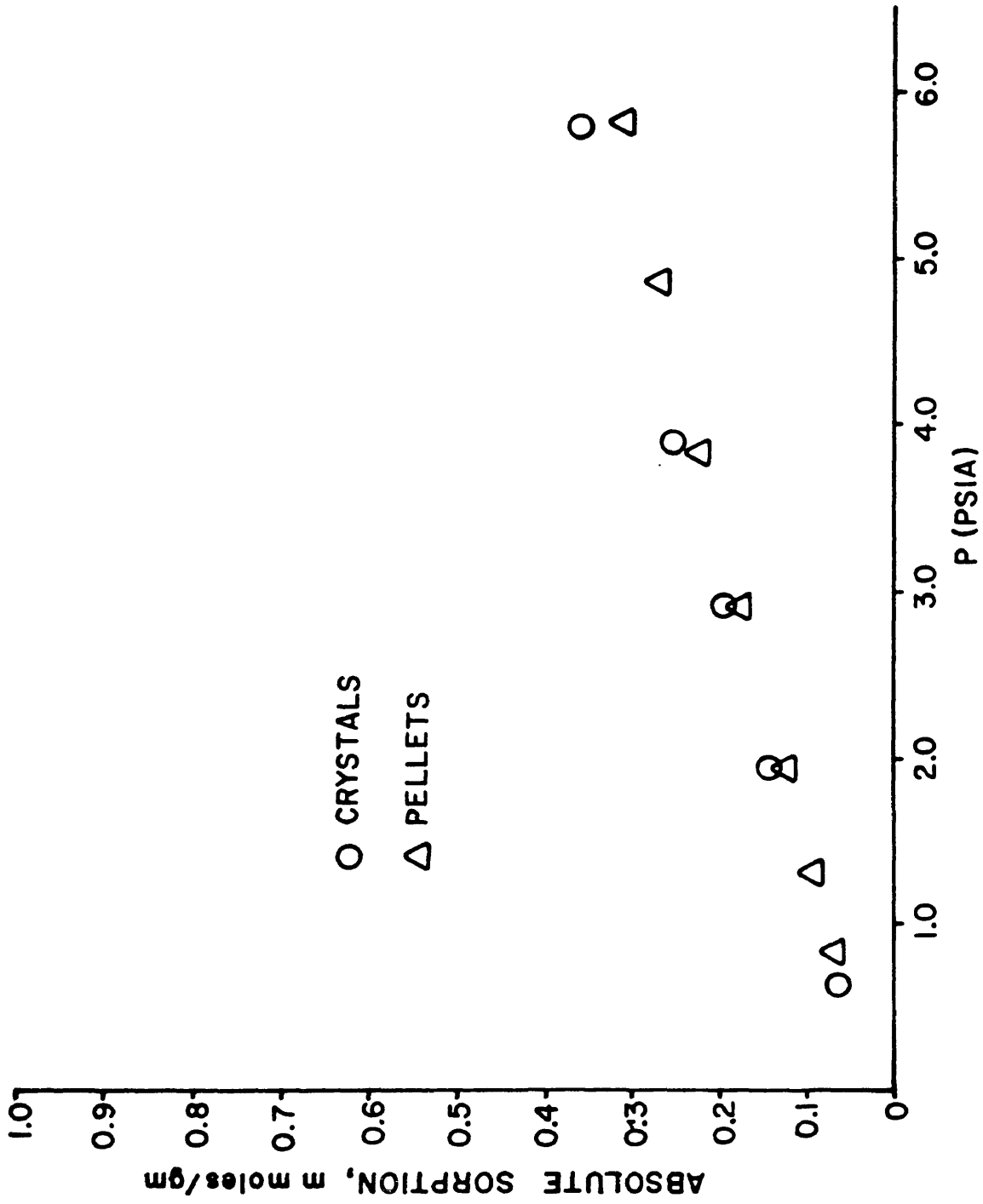


Figure 16. Comparison of Methane Adsorption Isotherms on 5A Crystals and Pellets at 298°K.

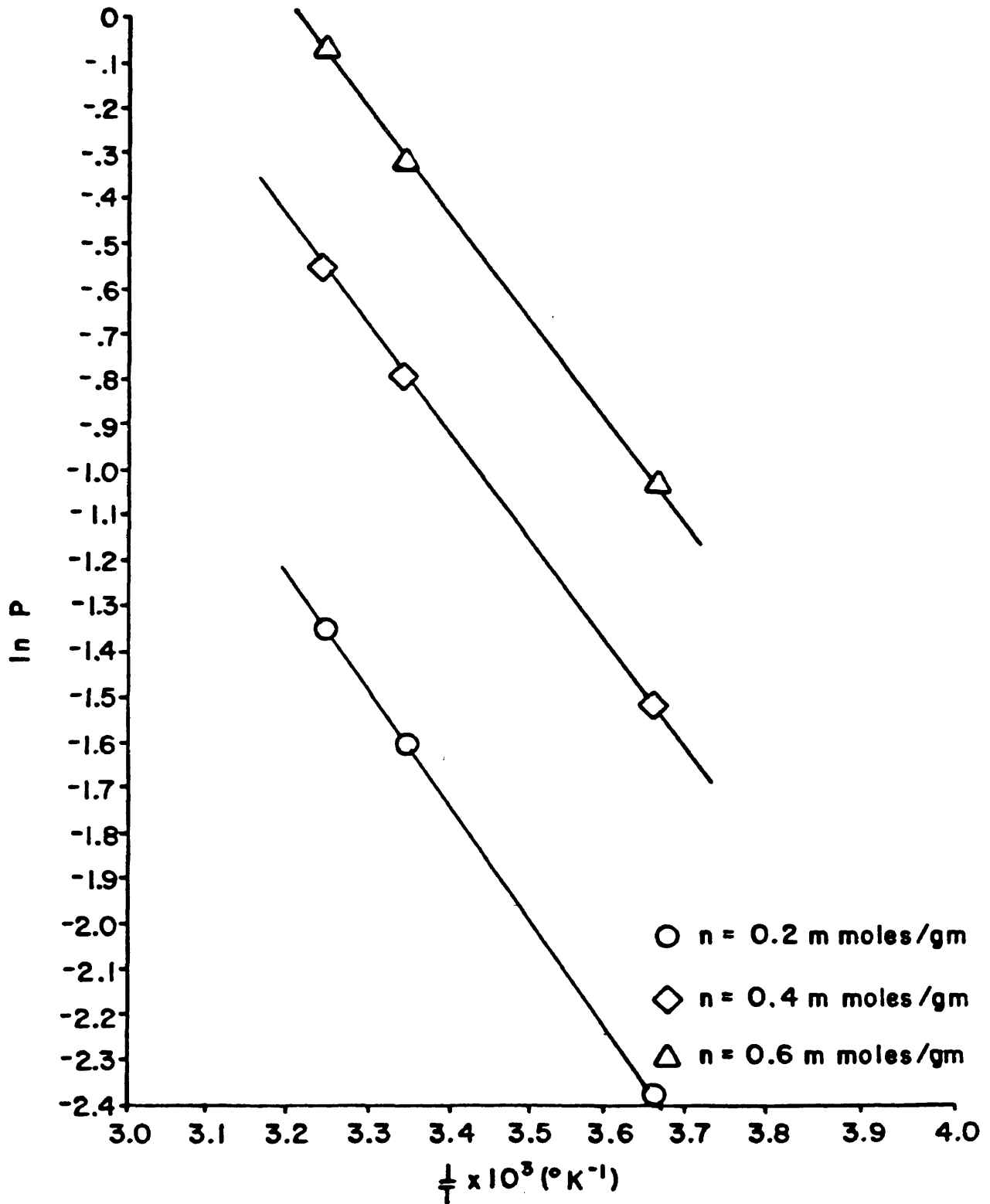


Figure 17. Adsorption Isotherms at Various Loadings.

Table 2
Variation of Isosteric Heat of
Adsorption with Loading

<u>Loading (mmoles/g)</u>	<u>q_{isos} (kcal/mole)</u>
0.2	-5.0
0.4	-5.0
0.6	-4.6
1.0	-4.3
1.5	-4.6
2.0	-4.9
2.25	-5.0

The characteristic curve for methane adsorption on 5A sieve is shown in Figure 18. The molar volume and saturation fugacity at each temperature must be known in order to determine the characteristic curve. Since the physical state of the sorbed species is considered to be essentially that of a liquid according to the Polanyi potential theory, it is logical to assume that the molar volume is the same as that of the corresponding liquid. At temperatures above the critical temperature, however, the effect of compressibility becomes large making the prediction of the molar volume of the sorbed species difficult. For this study, the molar volume was assumed to be constant and given a value of 50 cc/mole. This is the methane molar

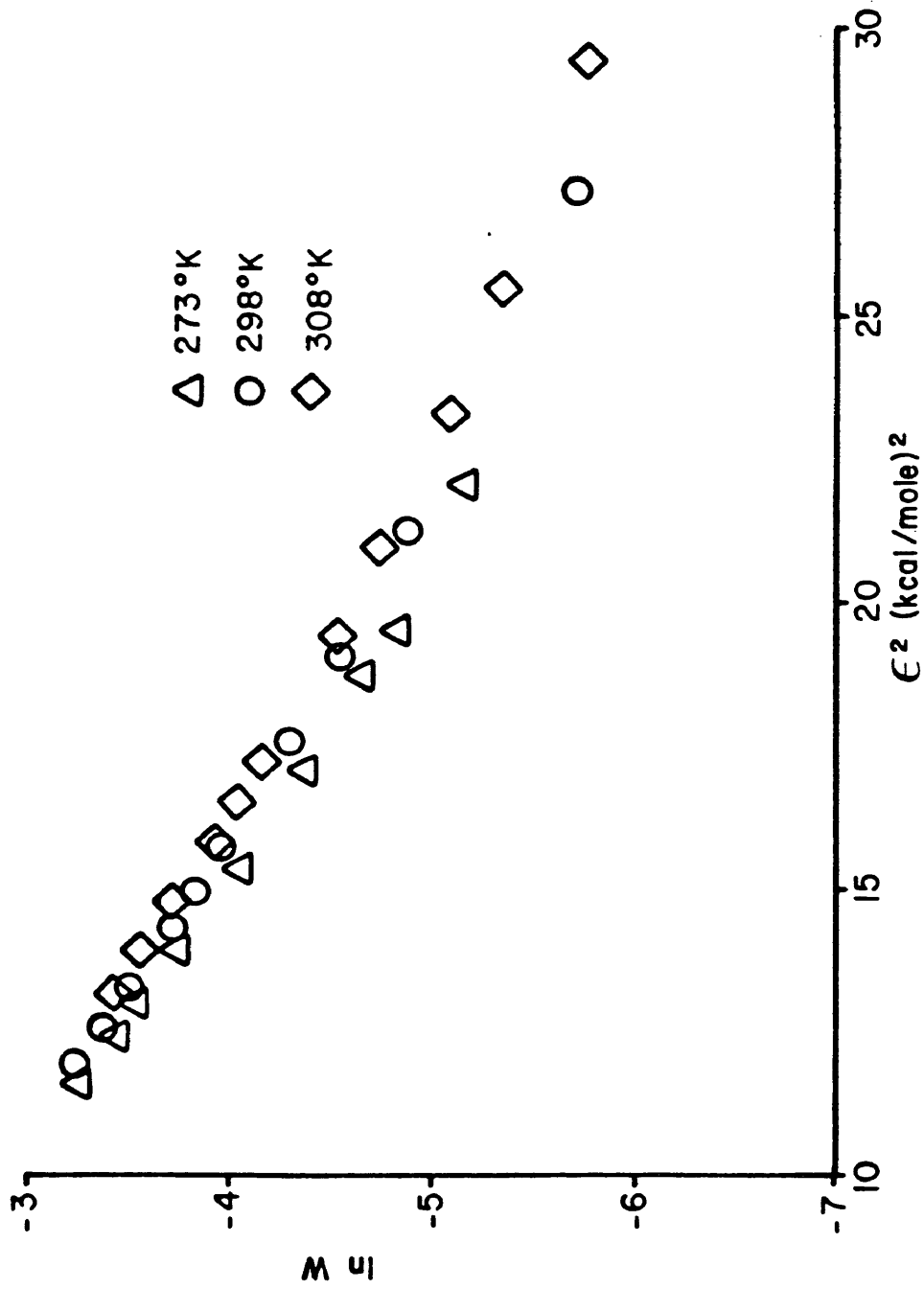


Figure 18. Characteristic Curve Plotted in the Form $\ln W$ Versus ϵ^2 for Methane Adsorption on 5A Crystals.

volume at 273°K determined by Loughlin (4). Ruthven and Loughlin (6) found that if a constant effective volume is assumed at supercritical temperatures that their model predicts a constant isosteric heat of adsorption. The saturation fugacity was calculated by extrapolation on the basis of the Clausius Clapeyron equation. Figure 19 is a plot of the test used to determine the fit of the data to the BET isotherm equation. A line was drawn through the points so that the surface area could be roughly approximated. This analysis yielded a surface area of 867 meters squared per gram. The monolayer loading can be approximated by assuming a molar volume of 50 cc/mole. The monolayer loading determined in this manner is 8.2 mmoles/gm. The Langmuir and Freundlich tests are applied in Figures 20 and 21. An attempt is made to fit the data using Ruthven's parameters in Figures 22 and 23 to first the low and then the high pressure data.

Once a value of K is determined from the data it is just a matter of finding a b value that gives a good fit by trial and error.

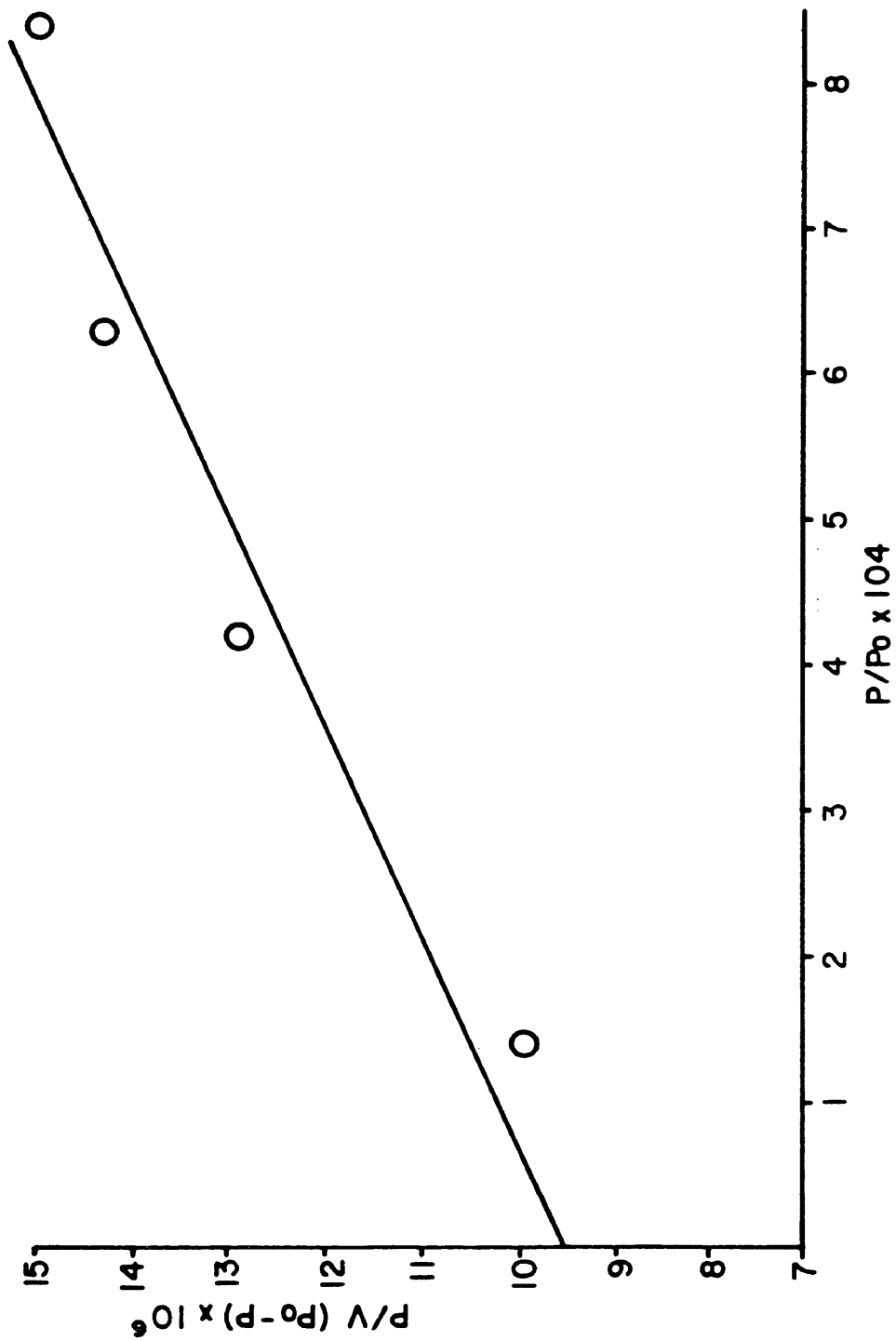


Figure 19. Plot of $P/V (P_0 - P)$ Versus P/P_0 for 298°K Data on 5A Crystals (Test for BET Isotherm Fit).

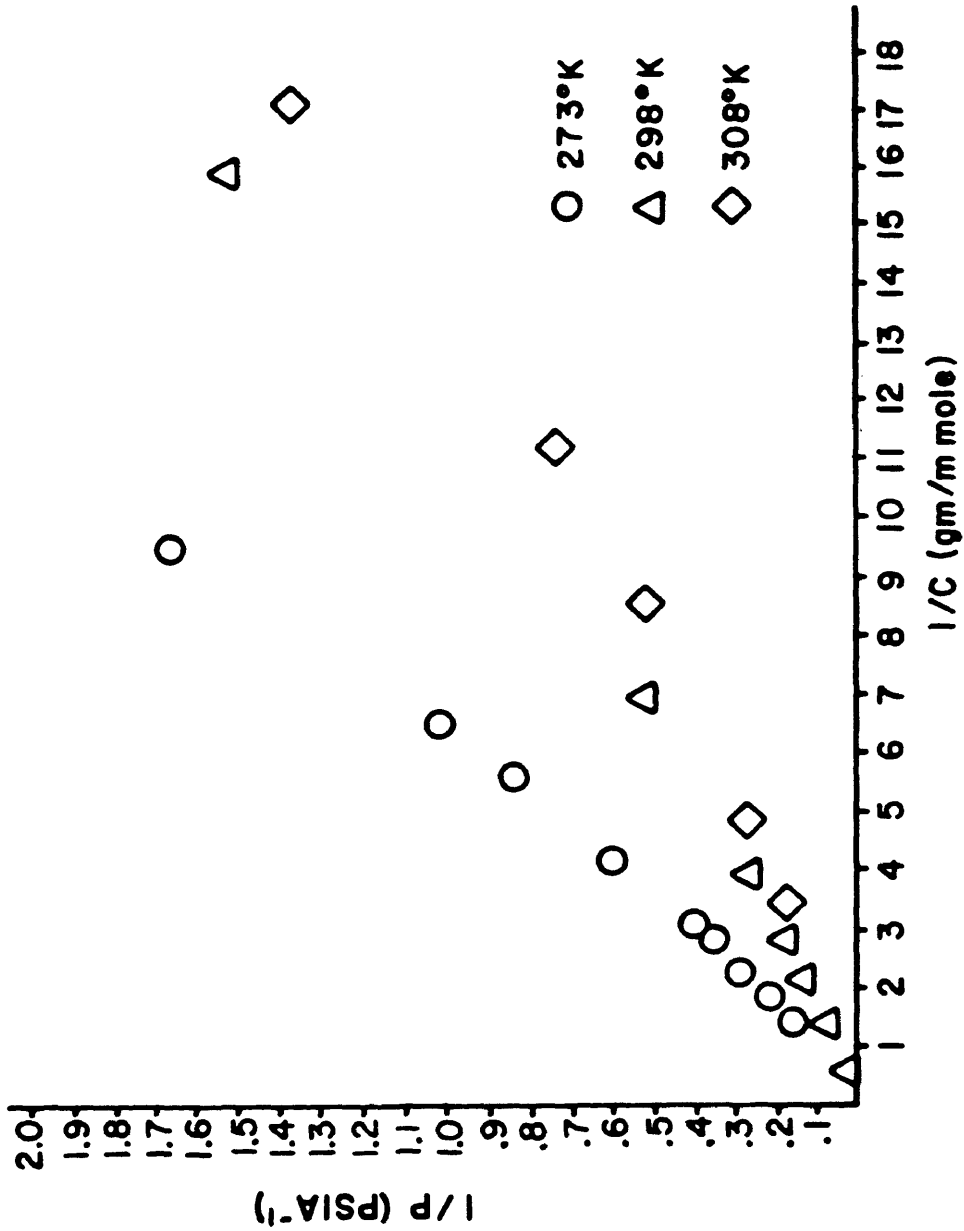


Figure 20. Plots of 1/P Versus 1/C for 273, 298, and 308°K Data on 5A Crystals (Test for Langmuir Isotherm Fit).

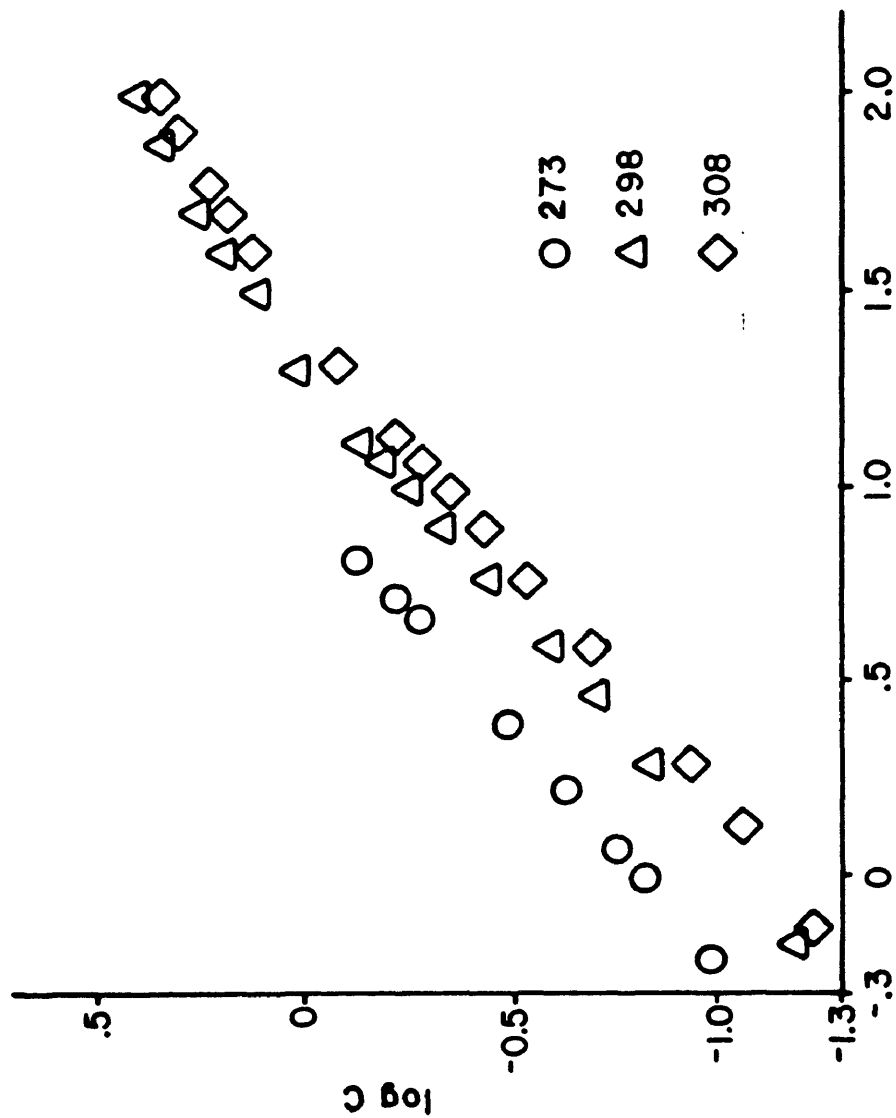


Figure 21. Plots of Log C Versus Log P for 273, 298, and 308°K Data on 5A Crystals (Test for Freundlich Isotherm Fit).

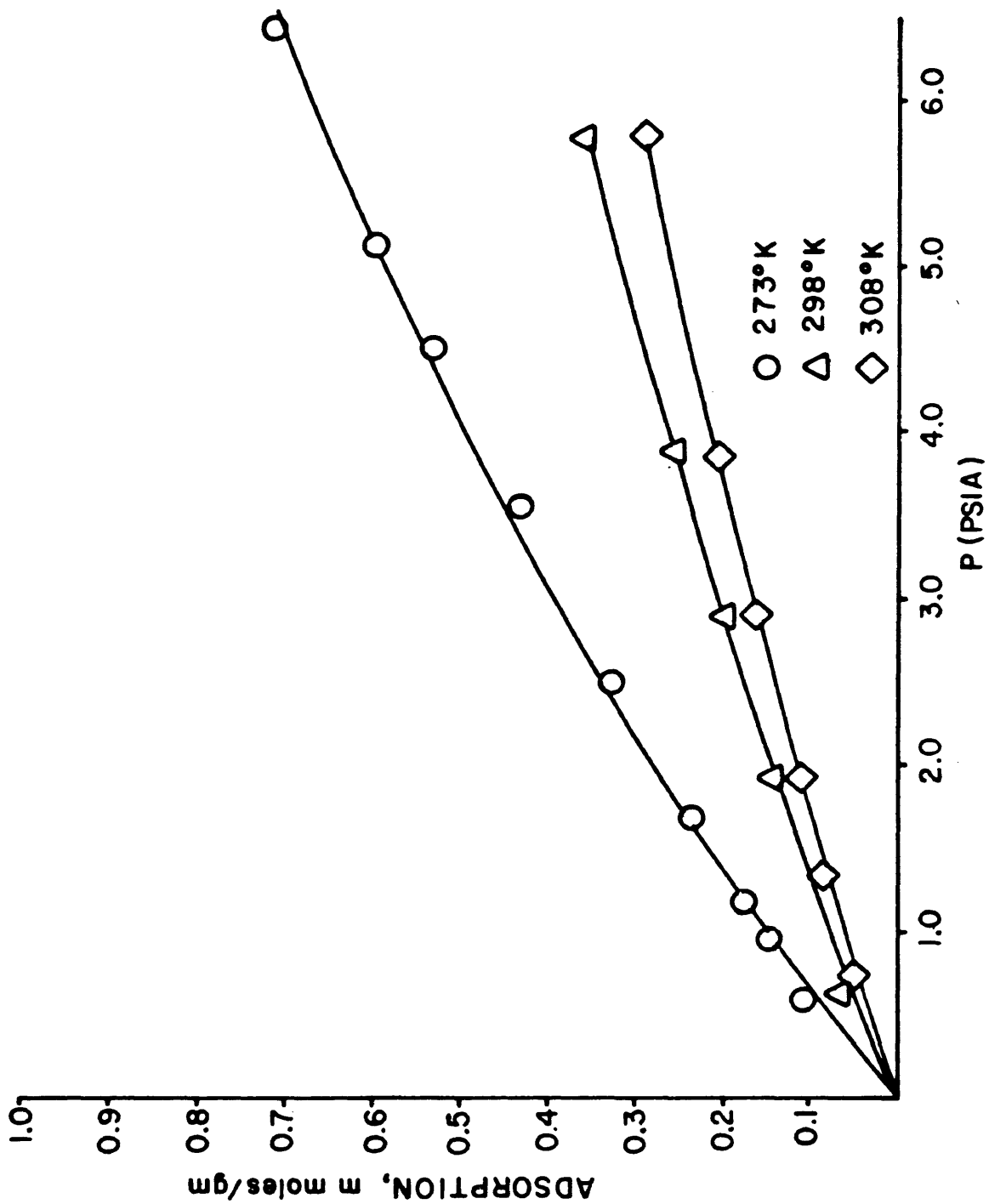


Figure 22. Low Pressure Isotherms Fit by Ruthven's Model.

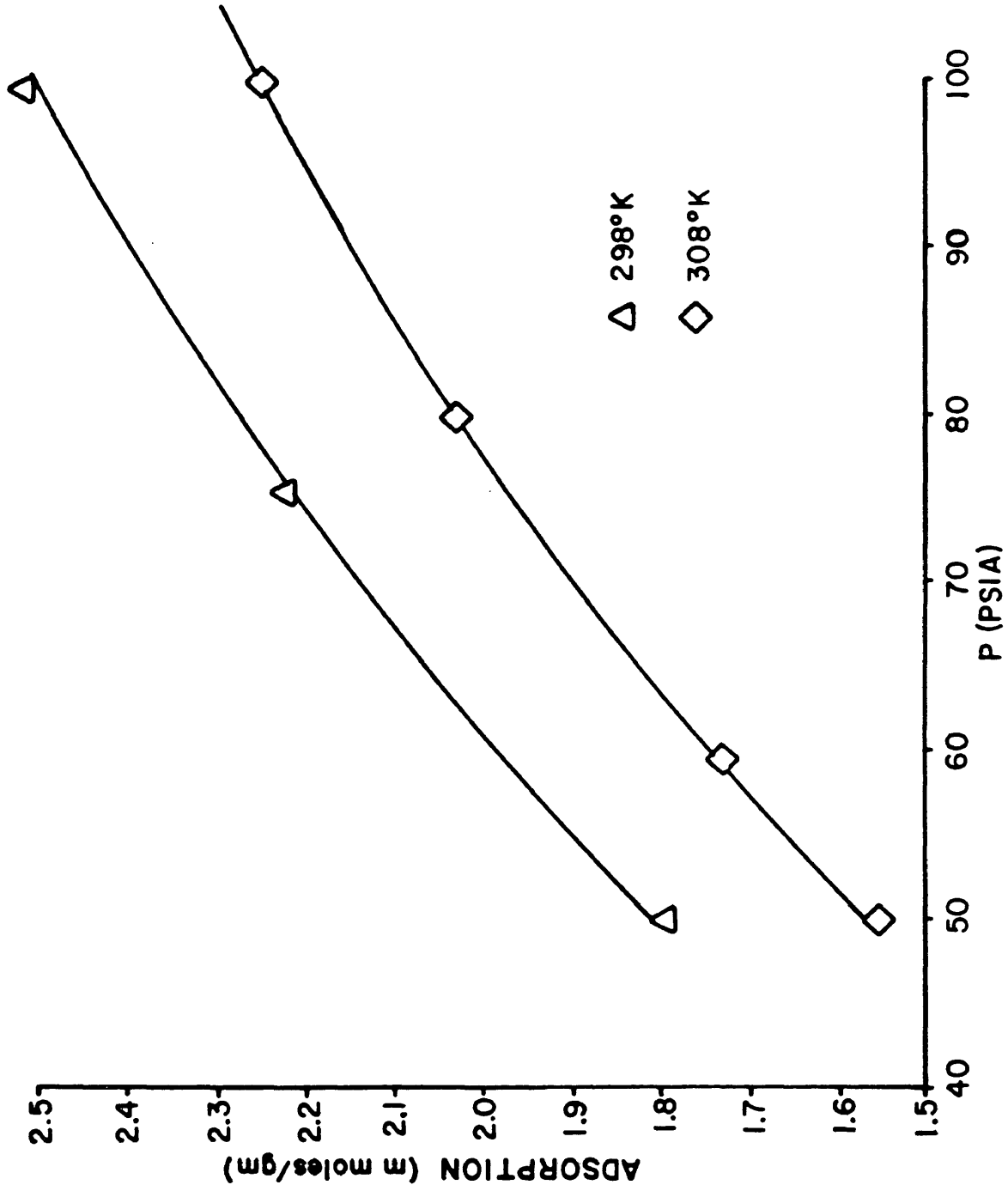


Figure 23. High Pressure Isotherms Fit by Ruthven's Model.

DISCUSSION

The lack of any apparent hysteresis for the isotherms at 273, 298, and 308°K shown in Figures 12, 13, and 14 suggests that all isotherm points were measured at pressure and temperature equilibrium. All the data points lie on a fairly smooth curve that can be extrapolated through the origin.

The adsorption isotherms at 273 and 298°K for both the 5A pellets (or powder) and the crystals shown in Figures 15 and 16 become essentially coincident provided that sorbate concentrations for pellets are corrected by a factor of 1/0.85. This is done to allow for the presence of approximately 15 weight percent inert clay binder.

The methane adsorption isotherm on 5A zeolite at 273°K is compared with the data of Loughlin (22) in Figure 24. The isotherm lies as much as 14^{1/2} percent below Loughlin's. Loughlin's data does not seem to fit a smooth curve passing through the origin. The incongruity in the two isotherms is difficult to explain considering the determinations were conducted in a similar manner on pure crystals from the same lot.

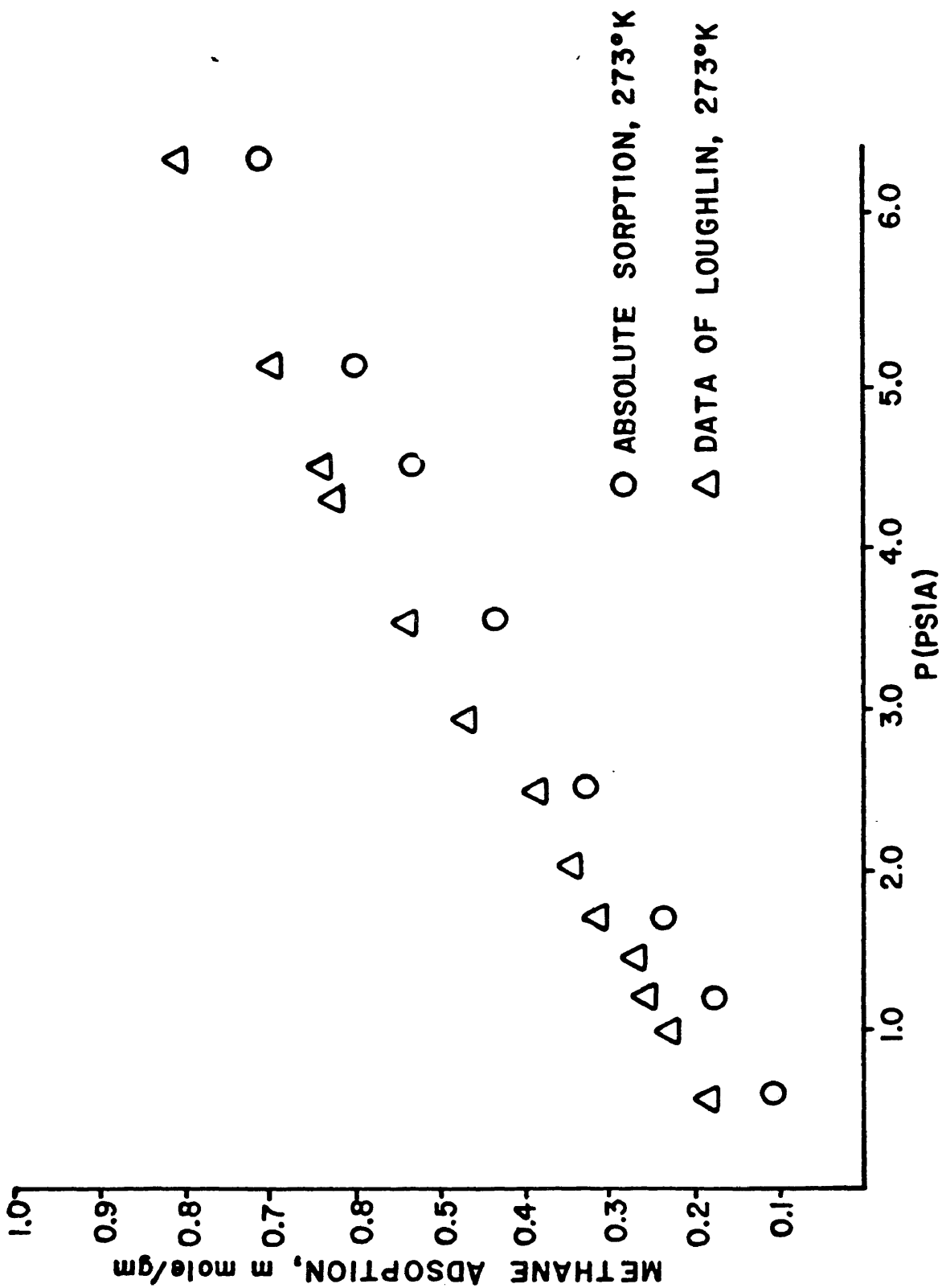


Figure 24. Comparison of 273°K Isotherm Data on 5A Crystals.

Table 3 compares the 298 and 308°K isotherm data with the pellet data of Rolniak corrected for the presence of 20% inert clay binder (9).

Table 3

Comparison of High Pressure

Data with Rolniak's Data

Temperature (°K)	Pressure (psia)	Adsorption (mmoles/g)		% Deviation
		This Study	Rolniak	
298	50.0	1.795	1.968	-8.8
	100.0	2.520	2.730	-7.7
308	50.0	1.556	1.674	-7.0
	100.0	2.253	2.469	-8.7

The results indicate that isotherms of this study lie between 7 and 9 percent below Rolniak's results. The differences are not completely unexpected considering the differences in samples and methods.

The isosteres in Figure 17 indicate that the data is internally consistent. All the points seem to lie on straight lines. The relatively invariant heat of adsorption for the methane - 5A system indicates the homogeneity of the 5A surface. The isosteric heat of sorption of methane derived from the isotherm data (5.0 Kcal/mole) agrees well with Ruthven's value of 5.1 kcal/mole (10). Rolniak reports

values at higher loading ranging from 3.7 to 3.9 kcal/mole (9).

Figure 18 indicates that the data comes relatively close to lying on a characteristic curve and any deviations may be due to the extrapolations used to determine the saturation fugacities. Notice that the closer the temperatures, the closer the curves are to one another.

Loughlin attempted to show the internal consistency of his data using a characteristic curve. An extrapolation technique was used to determine the molar volumes as a function of temperature. He made no attempt to show the internal consistency of his 273°K data with his lower temperature data by applying the more straight-forward isostere plots.

The plot of $P/V(P_0 - P)$ versus P/P_0 in Figure 19 does not yield a straight line and, therefore, the data cannot be fit very well by a BET isotherm equation. The surface area determined using the straight-line through the data, 867 m²/g, is larger than the surface area reported by Kidnay and Hiza, 506 m²/g. Some of the discrepancy is due to the presence of clay binder in the pellets of Kidnay and Hiza. The monolayer loading determined, 8.2 mmoles/g, suggests that all the isotherms were determined at below monolayer coverage.

As far as is known, no satisfactory model has been developed to fit the methane adsorption data of 5A zeolite over the entire pressure range of this study.

The deviation of the plots in Figures 20 and 21 from linearity indicates that the data cannot be fit by the simple Langmuir and Freundlich isotherm models over the entire pressure range. Ruthven's model fits the data points to within 6 percent except for the lower pressure data points as can be seen in Figures 22 and 23. Table 4 gives the values of K and b used to fit the isotherm data over these pressure ranges and compares them with those obtained by Laughlin and Rolniak.

All of the values seem to be reasonable except for Rolniak's Henry's law constant for the high pressure data at 308°K. Rolniak's value for K does not seem to be decreasing with increasing temperature as it should. This inconsistency may be seen more clearly, perhaps, by examining Figure 25.

An attempt was made to predict the effective molecular volume for the middle pressure region using the b values obtained in the high and low pressure regions. The effective molecular volume as a function of pressure at 298°K was found to be

$$b = 91.7 (P)^{-0.091} \quad (10)$$

where P in this case is the average pressure in the middle pressure region, 27.5 psia. Similarly, at 308°K

$$b = 101.7 (P)^{-0.111} \quad (11)$$

Table 4

Comparison of the Statistical Thermodynamics
 Model Parameters Determined from
 the Data of this Study with Those
 Obtained from the Data of Loughlin
 and Rolniak

Low Pressure Parameters

<u>T (°K)</u>	<u>K(molecules/cavity torr)</u>	<u>b(Å³/molecule)</u>
190	0.33	57.5
212	0.083	64.5
230	0.033	64.5
253	0.011	64.5
273	0.007	77
273*	0.006	80
298*	0.003	83
308*	0.002	90

High Pressure Parameters

<u>T(°K)</u>	<u>K(molecule/cavity psia)</u>	<u>b(Å³/molecule)</u>
298	0.1706(0.003)	60-62
298*	0.1400(0.003)	62
308	0.2300(0.004)	60-62
308*	0.1110(0.002)	63

* this study.

Quantities in parenthesis represent K in units of molecules/
 (cavity·torr)

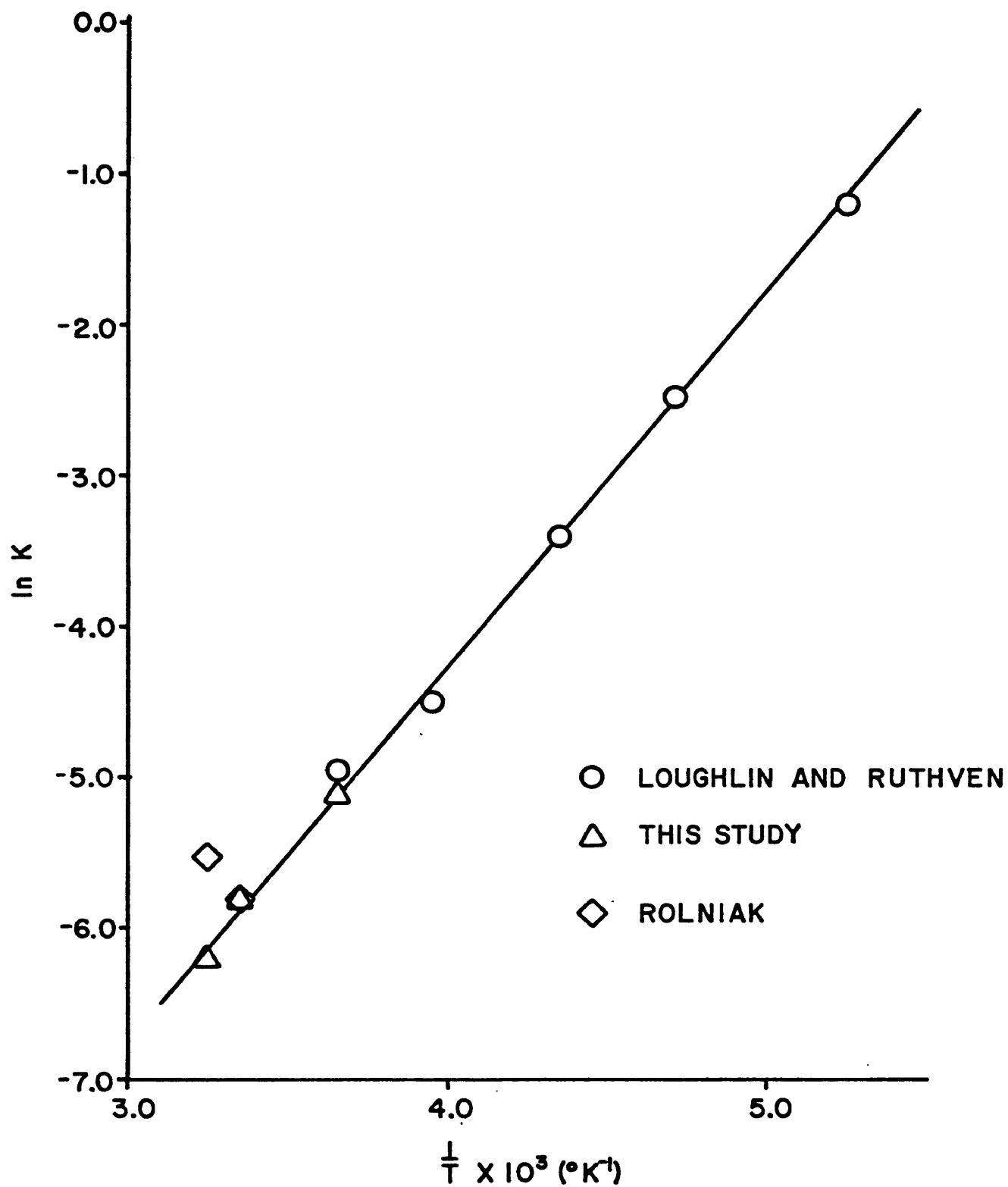


Figure 25. Plot of $\ln K$ vs. $1/T$ Used to Compare Henry's Law Constants.

The values for the effective molecular volume determined in this manner are 68 and 70 Å³/molecule at 298 and 308°K, respectively. Figure 26 shows the fits obtained using these volumes. The deviation is less than 5 percent.

The above equations were then used in an effort to fit the data over the entire pressure range. By simply inserting equations 10 and 11 into equation 7, a good fit of the data at 298 and 308°K was found over the entire pressure range as shown in Figures 27 and 28. The deviation between the data and the fit was less than 2 percent.

ARTHUR LAKES LIBRARY
COLORADO SCHOOL of MINES
GOLDEN, COLORADO 80401

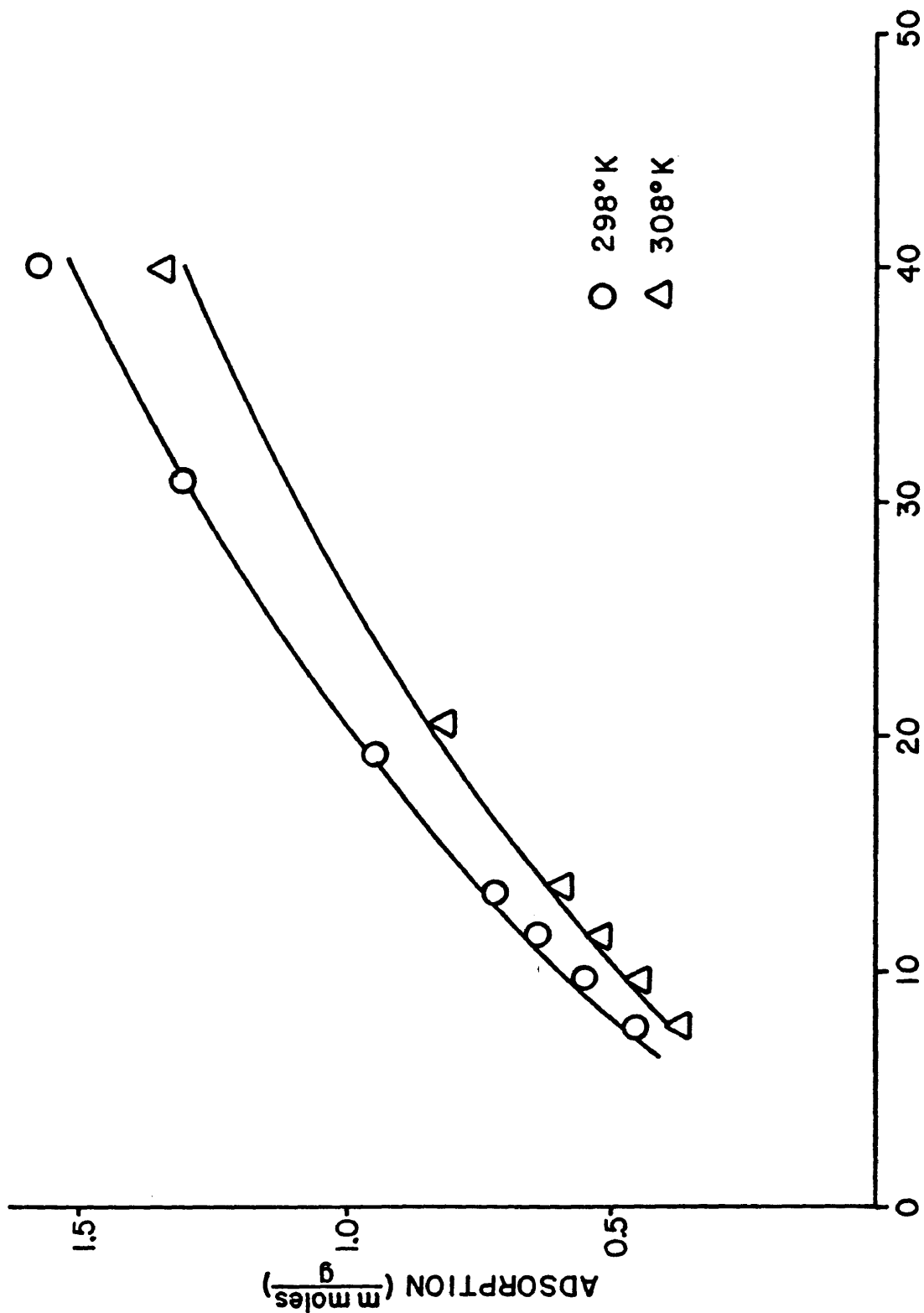


Figure 26. Middle Pressure Range Isotherms Fit by Ruthven's Model.

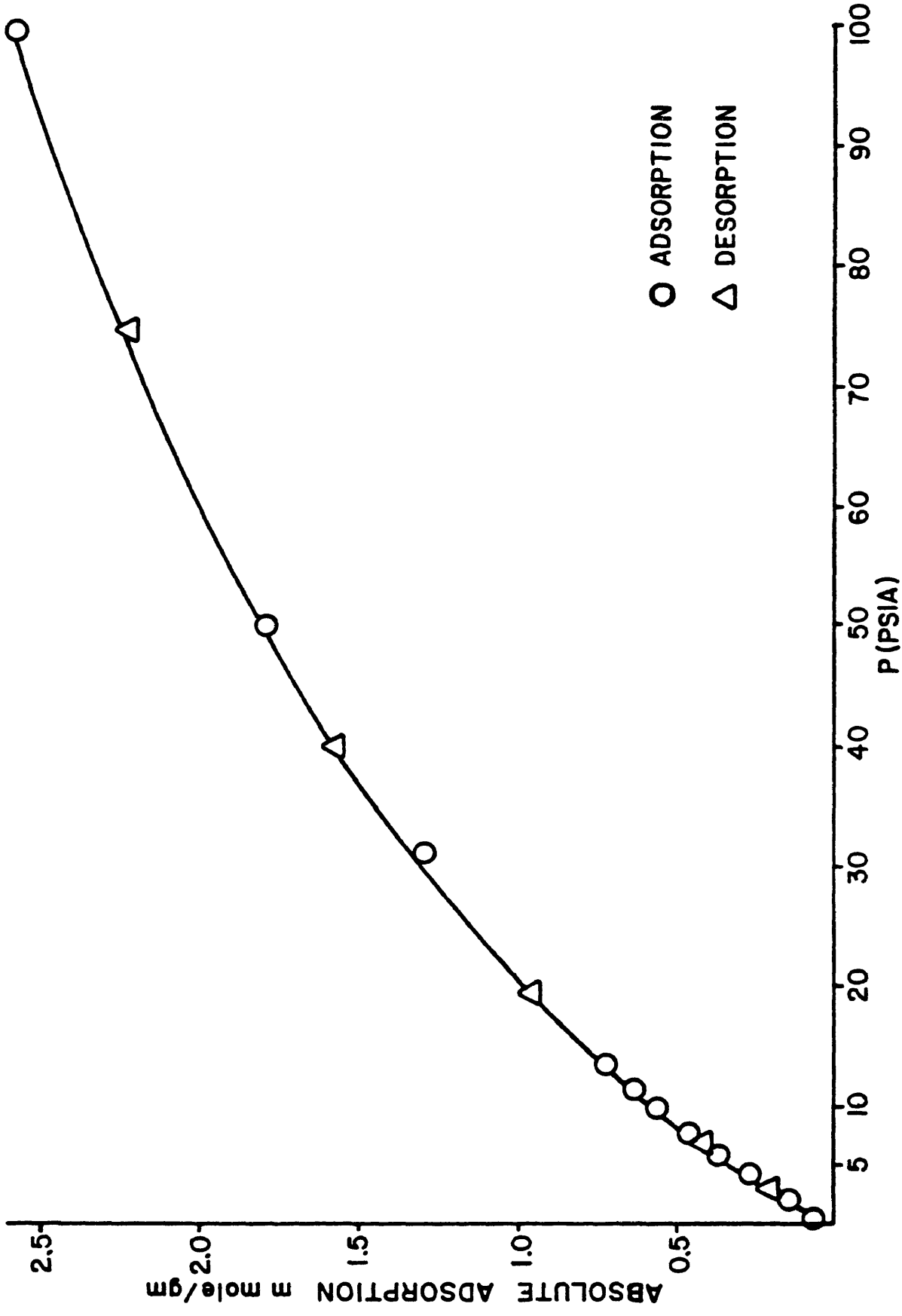


Figure 27. Methane Adsorption on 5A Crystals at 298°K Fit with Ruthven's Model Using Effective Molecular Volume-Pressure Relationship Determined from this Study.

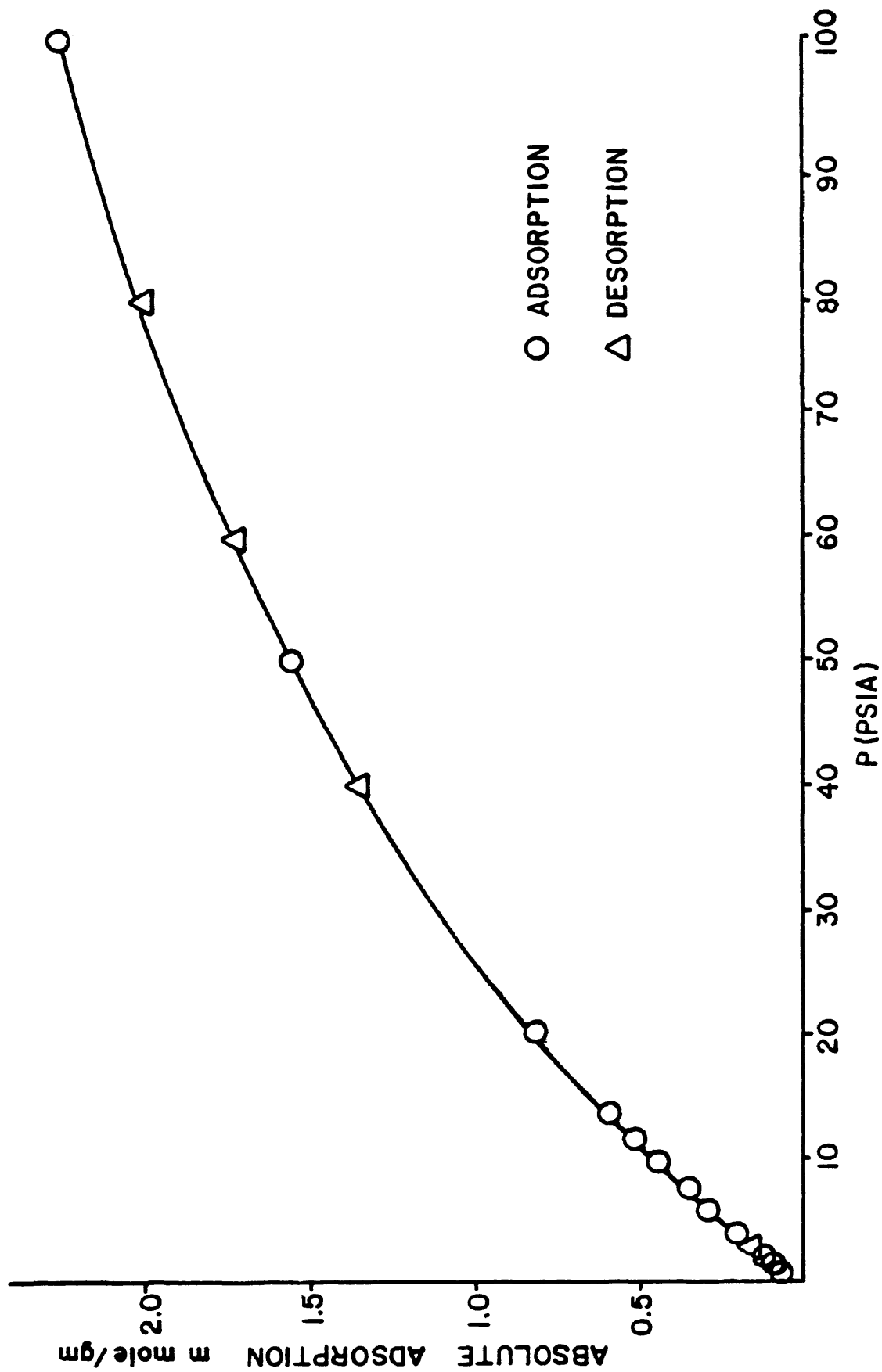


Figure 28. Methane Adsorption on 5A Crystals a 308°K Fit with Ruthven's Model Using Effective Molecular Volume-Pressure Relationship Determined from this Study.

CONCLUSIONS

The basic conclusion of this work is that a static adsorption apparatus capable of measuring accurate adsorption isotherms has been designed and constructed. Methane adsorption on Linde 5A zeolite has been measured at 273, 298, and 308°K. Equilibrium was achieved for each run based on the lack of hysteresis.

The isosteric heat of adsorption studies indicate that the data is internally consistent. The relatively constant isosteric heats of adsorption at various amounts adsorbed indicate that the sorbent surface is fairly homogeneous.

Difficulty is encountered in applying the Dubinin-Polanyi theory to methane adsorption on 5A zeolite at the isotherm temperatures of this study. Molar volumes and saturation fugacities at temperatures above the critical temperature are difficult to predict.

The BET surface area approximation along with the Loughlin's molar volume prediction indicates that the surface coverage was well below monolayer coverage for the adsorption runs.

The pellets and powder used in this study contain about 15 weight percent clay binder that acts as an inert diluent.

The data obtained cannot be fit over the entire pressure region using the Freundlich or Langmuir equations. The data can be fit by the Ruthven model if the relationships between the effective molecular volume and pressure found in this study are used.

RECOMMENDATIONS

1. Enclose entire apparatus and temperature control the enclosure.
2. Duplicate runs on the adsorbent to be used should be made with and without the liquid nitrogen trap to determine if it is really a necessary part of the apparatus.
3. Bouyancy tests should be conducted after an isotherm is determined so that the volume of the glass beads can be more closely matched to the volume of the regenerated sample.

APPENDIX A

Table AI

Adsorption of Methane
on 5A Crystals (Run 16)

Temperature: 273°K

<u>p (psia)</u>	<u>Adsorption (mmoles/g)</u>
0.600	0.105
0.983	0.152
2.509	0.326
4.528	0.530
6.437	0.714
5.164	0.596
3.559	0.434
2.524	0.328
1.696	0.236
1.191	0.177

Table AII
Adsorption of Methane
on 5A Crystals (Run 17)

Temperature: 298°K

<u>P (psia)</u>	<u>Adsorption (mmoles/g)</u>
0.654	0.063
1.994	0.143
3.901	0.254
5.781	0.356
7.733	0.454
9.816	0.552
11.657	0.637
13.518	0.719
31.1	1.313
50.0	1.795
99.6	2.515
75.3	2.225
40.2	1.583
19.3	0.947
6.795	0.407
2.909	0.197

Table AIII
Adsorption of Methane
on 5A Crystals (Run 18)

Temperature: 308°K

<u>P (psia)</u>	<u>Adsorption (mmoles/g)</u>
0.727	0.058
1.352	0.088
1.938	0.116
3.870	0.204
5.812	0.288
7.748	0.369
9.671	0.446
11.569	0.518
13.692	0.599
20.6	0.815
50.0	1.556
100.0	2.253
80.1	2.026
59.6	1.732
40.0	1.348
6.791	0.332
2.905	0.164

Table AIV
Adsorption of Methane
on 5A Powder (Run 12)

Temperature: 273°K

<u>P(psia)</u>	<u>Adsorption (mmoles/g)</u>
0.847	0.120
2.516	0.282
4.518	0.444
6.393	0.578
5.189	0.494
4.321	0.430
3.567	0.372
2.944	0.321
2.532	0.286
2.031	0.241
1.700	0.210
1.426	0.183
1.184	0.158

Table A.V.

Adsorption of Methane
on 5A Pellets (Run 15)

Temperature: 298°K

<u>P (psia)</u>	<u>Adsorption (mmole/g)</u>
0.843	0.0666
1.306	0.0939
1.959	0.125
2.915	0.176
3.843	0.219
4.865	0.266
5.818	0.307
6.785	0.348
7.758	0.387
8.714	0.424
10.029	0.473
11.064	0.510
11.878	0.538
11.762	0.534
13.567	0.595
19.9	0.784
40.0	1.243
59.9	1.545
79.9	1.771
99.7	1.957
50.1	1.418
13.443	0.591
10.462	0.489
7.678	0.389
5.824	0.310
3.884	0.224
1.934	0.127

Table A.VI

Bouyancy Test at 273°K

<u>Mass(mg)</u>	<u>Pressure (psia)</u>	<u>$\rho_G(g/cc) \times 10^5$</u>	<u>b' (mg)</u>	<u>c (μg)</u>
391.193	0.000	0.000	0.000	0
391.176	0.215	1.043	-0.017	14
391.175	0.602	2.923	-0.018	9
391.168	0.986	4.793	-0.025	10
391.168	1.433	6.965	-0.025	4
391.166	1.787	8.686	-0.027	0
391.158	2.338	11.366	-0.035	0
391.149	2.923	14.206	-0.044	0
391.136	3.934	19.127	-0.057	-2
391.120	4.928	23.964	-0.073	-1
391.116	5.777	28.096	-0.077	-10
391.079	7.714	37.524	-0.114	-2
391.048	9.671	47.061	-0.145	0
391.021	11.607	56.500	-0.172	-2
390.987	13.553	65.992	-0.206	2
390.950	15.5	75.496	-0.243	10
390.876	20.9	101.887	-0.317	2
390.715	31.0	151.371	-0.478	11
390.569	40.7	199.047	-0.624	9
390.422	50.0	244.898	-0.771	15
390.262	60.2	295.346	-0.931	19
389.906	84.1	414.210	-1.287	8
389.668	100.0	493.801	-1.525	0

Table A.VII.

Bouyancy Test at 298°K

<u>Mass (mg)</u>	<u>Pressure (psia)</u>	<u>$\rho_G(g/cc) \times 10^5$</u>	<u>b' (mg)</u>	<u>c (μg)</u>
552.541	0.000	0.000	-.000	0
552.535	0.193	0.861	-0.006	3
552.532	0.609	2.712	-0.009	1
552.524	1.311	5.838	-0.017	-1
552.520	1.669	7.431	-0.021	-2
552.508	2.675	11.910	-0.033	-4
552.493	3.810	16.968	-0.048	-4
552.464	5.785	25.767	-0.077	-3
552.425	8.675	38.651	-0.116	-4
552.384	11.781	52.511	-0.157	-6
552.349	14.545	64.851	-0.192	-9
552.268	20.0	89.229	-0.273	-3
552.002	40.0	178.880	-0.539	-14
551.717	60.0	268.958	-0.824	-8
551.445	80.0	359.458	-1.096	-17
551.147	100.0	450.391	-1.394	0

Table A.VIII.

Bouyancy Test at 308°K

<u>mass (mg)</u>	<u>Pressure (psia)</u>	<u>ρ_g (g/cc) x10⁵</u>	<u>b' (mg)</u>	<u>c (μg)</u>
514.250	0.000	0.000	0.000	0
514.246	0.679	2.924	-0.004	-4
514.241	1.333	5.741	-0.009	-6
514.235	1.932	8.322	-0.015	-6
514.228	2.899	12.488	-0.022	-10
514.221	3.870	16.673	-0.029	-14
514.205	5.797	24.980	-0.045	-19
514.179	7.727	33.303	-0.071	-15
514.161	9.669	41.681	-0.089	-18
514.141	11.584	49.946	-0.109	-19
514.120	13.503	58.232	-0.130	-20
514.040	20.6	88.903	-0.210	-19
513.830	39.8	172.108	-0.420	-23
513.700	50.0	216.447	-0.550	-7
513.600	59.5	257.827	-0.650	-13
513.362	80.2	348.279	-0.888	-8
513.131	100.0	435.165	-1.119	0

APPENDIX B

Error Analysis

The error in measurement and control will be examined and compared. In determining an equilibrium isotherm, the temperature must be both measured and controlled. The pressure and the weight are the parameters that must be measured.

The bath temperature was controlled to within 0.1°C and measured to within 0.1°F. Ruthven's theoretical model was used to predict the effect a 0.1°C temperature increase would have on an equilibrium isotherm. The three parameters affected by temperature are the Henry's Law constant, fugacity, and the effective molecular volume. Table 4 presented Henry's Law constants and effective molecular volumes as a function of temperature (10). For this analysis, the effect of 0.1°C on the effective molecular volume was assumed negligible. To examine the effect of temperature on the Henry's Law constant, a plot of $\ln K$ versus $1/T$ was made and found to be fairly linear. A least squares fit of the data yielded

$$\ln K = 2458.21 (1/T) - 14.08$$

A change in temperature from 273.15°K to 273.25°K results in a change in the Henry's Law constant from 0.006217 to 0.006196 molecules/(cavity-torr). This is a 0.33 percent decrease in K .

The computer program used in evaluating Ruthven's model equation uses the temperature to determine the fugacity. Therefore, by inserting the new Henry's Law constant into the program, the error introduced by the temperature change can be deduced. The results show that for a pressure of 2.0 psia the change in temperature from 273.15 to 273.25°K causes the loading to change from 0.2406 to 0.2399 mmoles/gram. This represents an overall error due to temperature control of 0.29 percent.

The pressure measurement errors must be determined for two different regions. The pressure readings were accurate to approximately 0.5 torr (0.0097 psia) below 800 torr. This gauge was used to measure pressure between 0.677 and 14.7 psia. The error, therefore, ranges between 1.43 and 0.07 percent. The pressure range from 14.7 to 100 psia was measured with the 0 to 250 psia transducer, which has an accuracy of roughly 0.1 psia. The error ranges from 0.68 to 0.10 percent.

The error in weight readings is directly tied to the drift experienced with changes in balance temperature. During the regeneration of the sieve the balance temperature may become 1°C higher than room temperature. This temperature increase corresponds to a possible weight increase of 27 micrograms. The regenerated weight of the sieve is approximately one gram. Therefore, the error in the regenerated weight may be 0.0027 percent.

The loading (mmoles adsorbed per gram sorbent) is determined using the equation

$$c = \frac{(m_a - m_r)/M}{m_r}$$

where

c = loading in mmoles/gram

m_a = actual weight in grams

m_r = regenerated weight in grams

M = molecular weight in millimoles per gram.

This equation can be rearranged to give

$$c = m_a/(m_r M) - 1/M$$

This means that the calculated loading will be 0.0027 percent lower than the actual.

The error in weight measurements is relatively small compared to the temperature control and pressure measurement errors. The maximum error is encountered at low pressures (35 torr) where the error in pressure measurement can be as high as 1.43 percent and the error in loading due to bath temperature instability can be as high as 0.29 percent.

APPENDIX C

Sample Calculations

The sample calculations for the system illustrate the procedure for run 18 for the adsorption of methane on 5A zeolite at a pressure of 3.870 psia unless otherwise indicated.

Bouyancy Correction Calculation

$$b' = \frac{ms}{\rho_s} \cdot \rho_g - V_c \cdot \rho_g - C$$

$$\rho_g = \frac{PM}{ZRT}$$

$$Z = 1 + \frac{Pr}{Tr} \left(\frac{B \cdot Pc}{RTc} \right)$$

$$\frac{B \cdot Pc}{R \cdot Tc} = B^\circ + w B'$$

$$B^\circ = 0.083 - \frac{0.422}{T_r^{1.6}}$$

$$B' = 0.139 - \frac{0.172}{T_r^{4.2}}$$

$$M = 16 \text{ g/gmole}$$

$$Tc = 190.6^\circ\text{K}$$

$$Pc = 45.4 \text{ atm}$$

$$R = 82.06 \text{ atm}\cdot\text{cc/gmole}\cdot^\circ\text{K}$$

$$Tr = T/Tc = 308.15/190.6 = 1.62$$

$$Pr = P/Pc = 3.870/(14.7 \times 45.4) = 0.00580$$

$$B^\circ = 0.083 - 0.422/(1.62)^{1.6} = -0.112$$

$$B' = 0.139 - 0.172/(1.62)^{4.2} = 0.116$$

$$\frac{BPC}{RTC} = B^{\circ} + W \cdot B'$$

$$= -0.112 + (0.007)(0.116)$$

$$= -0.111$$

$$Z = 1 + 0.00580/1.62 (-0.111)$$

$$= 0.99996$$

$$\rho_g = \frac{(3.870)(16)}{(0.99996)(14.7)(82.06)(308.15)}$$

$$= 1.666 \times 10^{-4} \text{ g/cc}$$

$$V_C = \frac{ms}{\rho_s} - \frac{b'}{\rho_g}$$

$$= \frac{1.3151}{2.9447} + \frac{0.001119}{0.004352}$$

$$= 0.704 \text{ cc}$$

$$C = \left(\frac{ms}{\rho_s} - V_C \right) \rho_g - b'$$

$$= \left(\frac{1.3151}{2.9447} - 0.704 \right) (1.666 \times 10^{-4}) + 2.9 \times 10^{-5}$$

$$= -1.4 \times 10^{-5} \text{ g}$$

$$= -14 \mu\text{g}$$

$$m_a = m_m - b'$$

$$m_a = 3.154 + 0.029$$

$$= 3.183 \text{ mg}$$

Surface Area Calculation

The surface area is determined from the slope and the intercept of the line in Figure 20 using the procedure of Smith (24)

$$I = 9.5 \times 10^{-5}$$

$$s = 5.33 \times 10^{-3}$$

$$V_m = \frac{1}{I+s} = 184.3 \text{ cc/g}$$

$$S_g = \left[\frac{V_m \cdot N_O}{V_s} \right] \alpha$$

$$\alpha = 1.09 \left[\frac{M}{N_O \cdot P} \right]^{2/3}$$

$$\alpha = 109 \left[\frac{16}{(6.02 \times 10^{23})(0.32)} \right]^{2/3}$$

$$= 1.75 \times 10^{-15} \text{ cm}^2/\text{molecule}$$

$$S_g = \left[\frac{(184.3)(6.02 \times 10^{23})}{22400} \right] 1.75 \times 10^{-15}$$

$$= 8.67 \times 10^6 \text{ cc/g}$$

$$= 867 \text{ m}^2/\text{g}$$

ARTHUR LAKES LIBRARY
 COLORADO SCHOOL of MINES
 GOLDEN, COLORADO 80402

Monolayer Coverage Calculation

$$\text{Monolayer Coverage} = \frac{(1.75 \times 10^{-15})(6.02 \times 10^{23})}{867}$$

$$= 8.2 \times 10^{-3} \text{ gmoles/g}$$

$$= 8.2 \text{ mmoles/g}$$

Calculation for Characteristic Curve Parameters (ϵ^2 and $\ln W$)

$$\Delta G = RT \ln f/f_s$$

$$f = \phi \cdot p$$

$$\ln \phi = P_r/T_r (B^\circ + \omega B')$$

$$\ln \phi = \frac{0.00580}{1.62} [-0.112 + (0.007)(0.116)]$$

$$\ln \phi = -4.05 \times 10^{-4}$$

$$\phi = 0.9996$$

$$f = (0.9996)(0.2633)$$

$$= 0.2632 \text{ atm}$$

$$f_s = 350.7 \text{ atm (from Clausius-Clapeyron Extrapolation)}$$

$$\frac{\Delta G}{R} = T \ln \frac{f}{f_s}$$

$$\frac{\Delta G}{R} = 308.15 \ln \frac{0.2632}{350.7}$$

$$\epsilon = \Delta G = (1.987)(-2.217 \times 10^3)(10^{-3})$$

$$= 4.405 \text{ kcal/mole}$$

$$\epsilon^2 = 19.41 \text{ (kcal/mole)}^2$$

$$W = c \cdot v$$

$$W = (0.2043)(50)(10^{-3})$$

$$= 0.01083 \text{ cc/g}$$

$$\ln W = -4.53$$

APPENDIX D

Calibration Reports



Aerospace Division
BOULDER COLORADO 80302

METROLOGY LABORATORIES

REPORT OF CERTIFICATION

PERFORMED FOR

COLORADO SCHOOL OF MINES

INSTRUMENT: DISCHARGE VAC GAGE MANUFACTURER: C.V.C.

MODEL: 6DH-100A SERIAL: 25154 OTHER IDENTITY: TAG WITH TUBE

P.O. NUMBER:

This is to certify that the instrument was calibrated in our Laboratory on June 27, 1977, and was found to be within manufacturer's specifications, or to the specifications as given below:

<u>PARAMETER</u>	<u>RANGE</u>	<u>MANUF.</u> <u>TOLERANCE</u>	<u>UNCERTAINTY</u>	<u>SPECIAL</u>
------------------	--------------	-----------------------------------	--------------------	----------------

Repairs to the Instrument were performed to correct deficiencies as noted:

COMMENTS:

CONDITION OF INSTRUMENT ON RECEIPT:

This will further certify that the test described above was performed using Standards traceable to the National Bureau of Standards

DATE: 28 June 1977

BY: M.R. Peterson
Engineering Supervisor
Metrology Laboratories

BBRC TEST NUMBER 4430 14436

DISCHARGE VACUUM GAUGE CALIBRATION CONDUCTED BY BALL
BROTHERS RESEARCH CORPORATION ON JUNE 24, 1977.

<u>Indicated Pressure (Torr)</u>	<u>Standard Pressure (Torr)</u>
8×10^{-7}	4.9×10^{-7}
2×10^{-6}	1.2×10^{-6}
6×10^{-6}	4.4×10^{-6}
1×10^{-5}	7×10^{-6}
4.9×10^{-5}	3.1×10^{-5}
1×10^{-4}	1.05×10^{-4}
1.3×10^{-4}	1.3×10^{-4}
8×10^{-4}	9×10^{-4}
7×10^{-3}	7×10^{-3}



Aerospace Division
BOULDER, COLORADO 80302

METROLOGY LABORATORIES

REPORT OF CERTIFICATION

PERFORMED FOR
COLORADO SCHOOL OF MINES

INSTRUMENT: THERMISTER VAC GAUGE MANUFACTURER: GENERAL ELECTRIC

MODEL: 22GC320 SERIAL: EM OTHER IDENTITY: _____

P.O. NUMBER: _____

This is to certify that the instrument was calibrated in our Laboratory on June 27, 1977, and was found to be within manufacturer's specifications, or to the specifications as given below:

<u>PARAMETER</u>	<u>RANGE</u>	<u>MANUF. TOLERANCE</u>	<u>UNCERTAINTY</u>	<u>SPECIAL</u>
------------------	--------------	-----------------------------	--------------------	----------------

Repairs to the Instrument were performed to correct deficiencies as noted:

COMMENTS:

CONDITION OF INSTRUMENT ON RECEIPT:

This will further certify that the test described above was performed using Standards traceable to the National Bureau of Standards

DATE: 28 June 1977

BY: M.R. Peterson
Engineering Supervisor
Metrology Laboratories

BBRC TEST NUMBER 4430 14437

GE THERMISTOR GAGE

TAG USERDA 6327

MICRON SCALES

<u>STANDARD PRESSURE</u>	<u>CHANNEL #1 (Cal 30)</u>	<u>CHANNEL #2 (Cal 26)</u>
4	4	2
26	26	22
46	56	50
79	92	86

GAGE CHANNELS REVERSED
(Cal 26)

4	7	(Cal 30)
---	---	-----------

TORR SCALES

	<u>(Cal 30)</u>	<u>(Cal 26)</u>
46 Microns	50	50
79 "	95	85
470 "	590	500
965 "	1250	1000
2.5 Torr	5.0	3.0
23 "	350	100
125 "	400	250
437 "	88 on Micron Scale	500
ATM-637 "	96 on Micron Scale	92 on Micron Scale

GAGE CHANNELS REVERSED
(Cal 26)

ATM-637 Torr	94 on Micron Scale	94 on Micron Scale
12 Torr	100	300
2 Torr	2.5	3.0

NOTE: This Gaging Circuit has a resistor and a thermistor built into each gage plug. Although the manufacturer controls these elements within a close tolerance there will be a difference when the plugs and transducers are interchanged. Primary calibration was made with channel #1 connected to the Cal 30 Transducer. Best accuracy for this type of circuit is limited to the 10 to 1000 Micron range.

CALIBRATION DATA

06/20/77
SERIAL # AB12779

SERIES 1500 DIAL INSTRUMENT
0.0 - 800.000 MM. HG, 0 C

TEST PRESSURE PSI	TEST PRESSURE MM. HG, 0 C	GAUGE READING MM. HG, 0 C	ERROR MM. HG, 0 C	ERROR %
0.500	25.9	25.7	-0.2	-0.025
1.500	77.6	77.5	-0.1	-0.013
3.500	181.0	181.2	0.2	0.025
5.500	284.4	284.6	0.2	0.025
7.500	387.9	387.8	-0.1	-0.013
9.500	491.3	491.0	-0.3	-0.037
11.500	594.7	594.7	0.0	0.0
13.500	698.1	698.5	0.4	0.050
14.700	760.2	760.1	-0.1	-0.013

THIS IS TO CERTIFY THAT MATERIALS AND PROCESSES INVOLVED IN THE MANUFACTURE AND VERIFICATION OF THE PRODUCT(S) INCLUDED IN THIS SHIPMENT COMPLY WITH THE CATALOG, DRAWING OR SPECIFICATION REFERENCED IN THE ORDER.

IT IS CERTIFIED FURTHER THAT THE CALIBRATION IS TRACEABLE TO THE NATIONAL BUREAU OF STANDARDS.

760.200

PENWALT
 **WALLACE & TIERNAN**
 DIVISION
 25 MAIN STREET, BELLEVILLE, NEW JERSEY 07109
 Form 3650

L-2052

Form 1
11-1944

UNITED STATES DEPARTMENT OF COMMERCE
WASHINGTON

National Bureau of Standards

Certificate

FOR

Set of Metric Weights

Class M

Submitted by

United States Department of the Interior,
Bureau of Mines,
Laramie, Wyoming.

RESULTS OF TEST

Designation	Apparent Mass vs Brass		True Mass		Volume at 20° C
	Correction	Value	Correction	Value	
(100 g)	0.0 mg	100.000 0 g	0.0 mg	100.000 0 g	11.96 cm ³
(50 g)	0.0 "	50.000 0 "	0.0 "	50.000 0 "	6.00 "
(20 g)	-0.18 "	19.999 82 "	-0.18 "	19.999 82 "	2.377 "
(10 g)	-0.08 "	9.999 92 "	-0.09 "	9.999 91 "	1.187 "
(10 g) ..	-0.08 "	9.999 92 "	-0.09 "	9.999 90 "	1.185 "
(5 g)	-0.08 "	4.999 92 "	-0.08 "	4.999 92 "	0.592 "
(2 g)	+0.04 "	2.000 04 "	+0.04 "	2.000 04 "	0.235 "
(2 g) ..	+0.04 "	2.000 04 "	+0.03 "	2.000 03 "	0.235 "
(1 g)	0.00 "	1.000 00 "	-0.01 "	0.999 99 "	0.116 "
(500 mg)	0.00 "	0.500 00 "	-0.042 "	0.499 958 "	
(200 mg)	0.00 "	0.200 00 "	-0.017 "	0.199 983 "	
(100 mg)	0.00 "	0.100 00 "	-0.009 "	0.099 991 "	
(100 mg) ..	-0.01 "	0.099 99 "	-0.021 "	0.099 979 "	
(50 mg)	-0.03 "	0.049 97 "	-0.033 "	0.049 967 "	
(20 mg)	0.00 "	0.020 00 "	+0.006 "	0.020 006 "	
(10 mg)	-0.01 "	0.009 99 "	-0.004 "	0.009 996 "	
(10 mg) ..	0.00 "	0.010 00 "	+0.001 "	0.010 001 "	
(5 mg)	-0.018 "	0.004 982 "	-0.017 "	0.004 983 "	
(2 mg)	-0.005 "	0.001 995 "	-0.004 "	0.001 996 "	
(2 mg) ..	+0.002 "	0.002 002 "	+0.003 "	0.002 003 "	
(1 mg)	-0.001 "	0.000 999 "	0.000 "	0.001 000 "	
(10 mg) ^	0.00 "	0.010 00 "	0.00 "	0.010 00 "	
(10 mg) ^	+0.01 "	0.010 01 "	+0.01 "	0.010 01 "	

For the Director

by *L. E. Macurdy*

L. E. Macurdy
Chief, Mass Section
Division of Weights and Measures.

Test completed: May 29, 1946

11-2/Tw 109443

Supplement to Certificate for Weights of Class M

Conditions of Test

All observations were made under the following atmospheric conditions: temperature 23° C to 24° C relative humidity 34% to 55% and barometer 748 mm to 756 mm

Certified volumes were determined by hydrostatic weighings, assuming that the weights have a coefficient of cubical expansion of per degree Centigrade.

In computing true mass values for those weights for which volumes were determined, these volumes were used for making the necessary allowance for differences in the buoyant effect of the air. In other cases the weights were assumed to have the densities indicated below.

Denomination	Material	Density
500 mg to 50 mg	Platinum	21.5 g per cm ³ at 0°C
20 mg to 1 mg	Aluminum	2.7 " " " " "

Apparent Mass vs. Brass

The values under this heading are on a different basis from those under the heading "True Mass", in that the former values are those that the weights appear to have when compared in air under normal conditions against normal brass standards without making corrections for the buoyant effect of the air. (The normal conditions used are a temperature of 20°C and an air density of 1.2 mg per cm³. Normal brass standards are those having a density of 8.4 g per cm³ at 0°C and a coefficient of cubical expansion of 0.000 054 per degree Centigrade.)

When these weights are used in weighings under the normal conditions, no error is introduced by using these apparent mass values and assuming the weights to be of normal brass. When they are used under conditions that depart from normal, the errors introduced by this procedure equal the difference between actual and normal air density multiplied by the difference between actual and normal volumes of the weights used.

Corrections

Both the correction and the value for each weight are shown on the certificate. It will be found to be more convenient in computations to employ the corrections rather than the actual values. Thus the sum of the corrections for the weights used in a weighing, when added algebraically to the sum of the nominal values of these weights, eliminates the errors of the weights. If only a certain fractional part of the value of a weight enters the final result (e.g. when a rider is employed) the same fractional part of the correction should be used.

Precision and Accuracy of Certified Values


Values given for weights of all denominations have been rounded off to the nearest unit in the last decimal place given. The values are correct within less than one in this decimal place.

Test No. Tw 109443

Set:

BIBLIOGRAPHY

- (1) Hines, A.L., and Sloan, E.D., Jr., "The Role of Spent Shale in Oil Shale Processing and the Management of Environmental Residues," Colorado School of Mines, Golden (1976).
- (2) Young, D.M., and Crowell, A.D., Physical Adsorption of Gases, Butterworth and Company, London, (1962).
- (3) Brunauer, S., The Adsorption of Gases and Vapors, Clarendon Press, Oxford, and Princeton University Press, Princeton (1945).
- (4) Loughlin, K.F., Ph.D. dissertation, University of New Brunswick, New Brunswick, Canada (1970).
- (5) Ruthven, D.M. and Loughlin, K.F., "The Sorption of Light Paraffins in Linde 5A Zeolite," J. Phys. Chem. Solids, 32 2451 (1970).
- (6) Ruthven, D.M. and Loughlin, K.F., "Sorption of Light Paraffins in Type-A Zeolites," J. Chem. Soc. Faraday Trans., 68, 696 (1972).
- (7) Kidnay, A.J. and Hiza, M.J., "The Adsorption of Methane and Nitrogen on Silica Gel Synthetic Zeolite and Charcoal," J. Phys. Chem., 67, 1725 (1963).
- (8) Lederman, P.B. and Williams, B., "The Adsorption of Nitrogen-Methane on Molecular Sieves," AIChE J., 10, 30 (1964).
- (9) Rolniak, P.D., Ph.D. Dissertation, Rice University, Houston, Texas (1976).
- (10) Ruthven, D.M. "Sorption of Oxygen, Nitrogen, Carbon Monoxide, Methane, and Binary Mixtures of These Gases in 5A Molecular Sieve," AIChE J., 22 (4), 753 (1976).
- (11) Langmuir, J., J. Amer. Chem. Soc., 40, 1368 (1918).
- (12) Hill, F.L., "Statistical Mechanics of Adsorption vs. Thermodynamics and Heat of Adsorption," J. Chem. Phys. 17, 520-535 (1948).

- (13) Polanyi, M., Verh. dtsch. phys. Ges, 16, 1012 (1914).
- (14) Polanyi, M., Verh. dtsch. phys. Ges. 18, 15 (1916).
- (15) Dubinin, M.M., Russ, J. Phy. Chem. (English Trans) 697 (1965).
- (16) Bering, B.P., M.M. Dubinin and V.V. Serpinski, "Theory of Volume Filling for Vapor Adsorption," J. Colloid & Interface Sci., 21 378-393 (1966).
- (17) Dubinin, M.M., "Theory of Physical Adsorption of Gases and Vapors and Adsorption Properties of Various Natures and Porous Structures," Izv. Akad. Nauk, SSSR, Otd. Khim. Nauk, 7, 1153-1161 (1960).
- (18) Dubinin, M.M. and V.A. Astakov: Developments of the Concepts of Volume Filling of Micropores in the Adsorption of Gases and Vapors by Microporous Adsorbents, Communication 1: Carbon Adsorbents, Izv. Akad. Nauk. SSSR, Ser Khim., 1, 5-11 (1971).
- (19) Williams, C.J., "A New Lease on Life for Gravimetric Adsorption," American Laboratory, (1969).
- (20) Breck, D.W., Zeolite Molecular Sieves, John Wiley & Sons, New York (1974).
- (21) Linde Molecular Sieves booklet.
- (22) Every, R.L., Dell' Osso, L. Jr., "A Surface Chemistry Study of the Methane-Coal Problem," Conoco Research Report (1971). 
- (23) Sloan, E.D., Ph.D. Dissertation, Clemson University, Clemson, South Carolina (1974).
- (24) Smith, J.M., Chemical Engineering Kinetics, McGraw Hill Book Company, New York (1970).